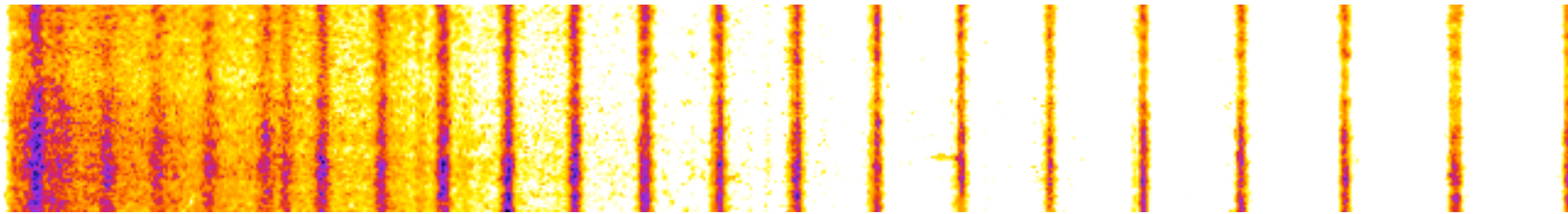


Ultrafast Laser-driven Probes for Investigating High Energy Density Physics

Franklin Dollar



High Energy Density (HED) Science Seminar Series
September 14, 2017 Lawrence Livermore

UCI University of
California, Irvine

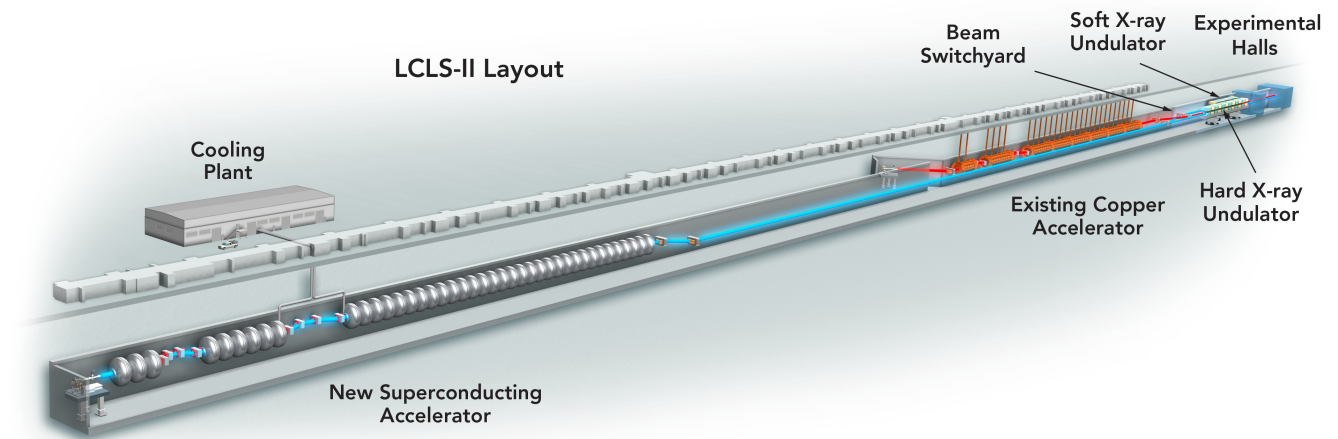
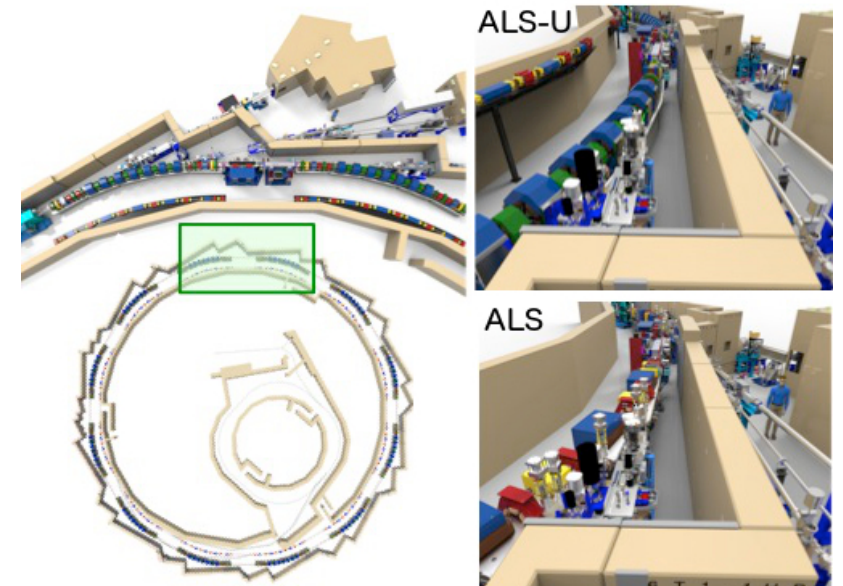
Outline

- Motivation
- MIR HHG
- UV HHG
- NC HHG
- Solid HHG
- Absorption
- MIR HHG
- Future work



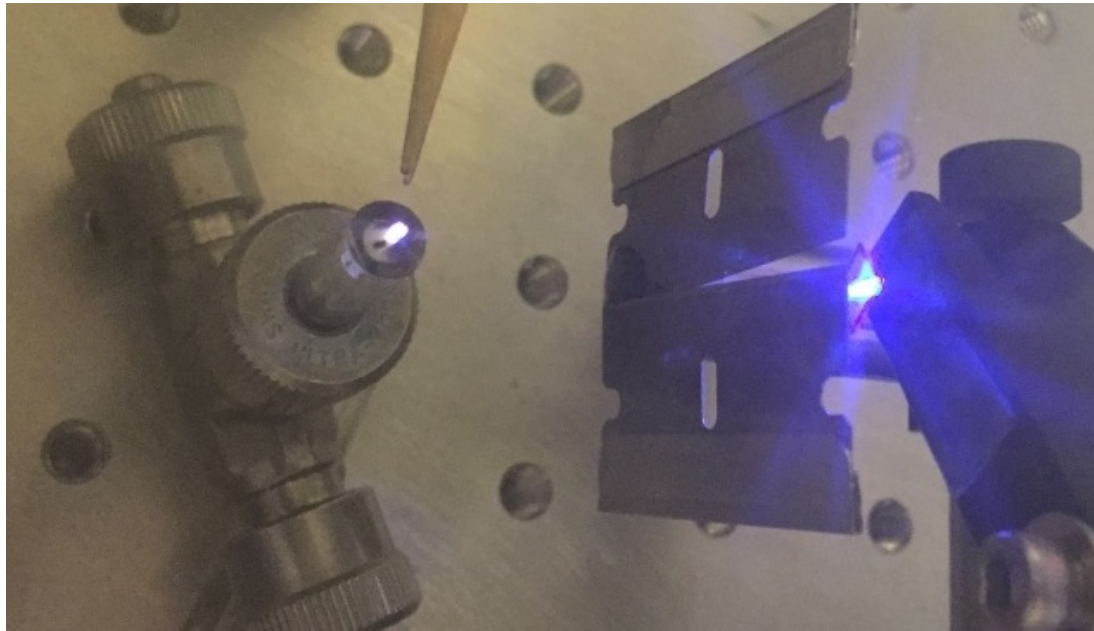
Coherent Light Sources

- Major infrastructure for coherent x-ray generation being developed
- Coherence enables novel imaging

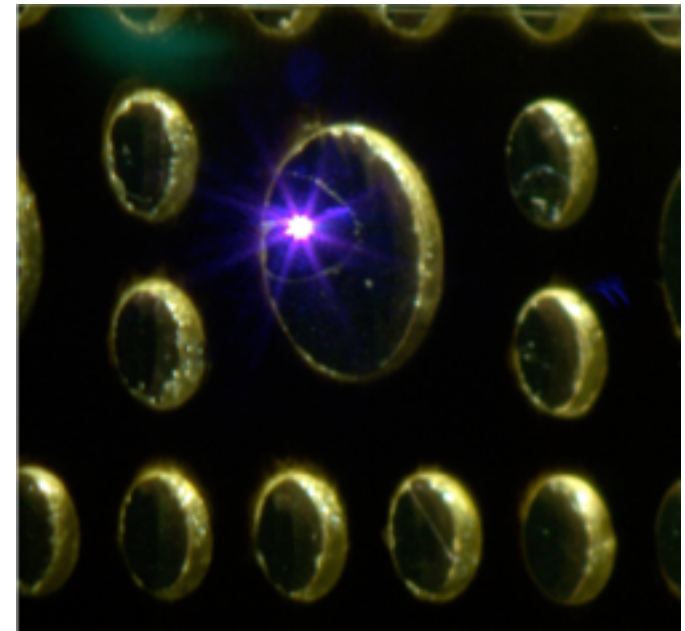


Laser Driven Coherent Light Sources

High harmonic generation (HHG)

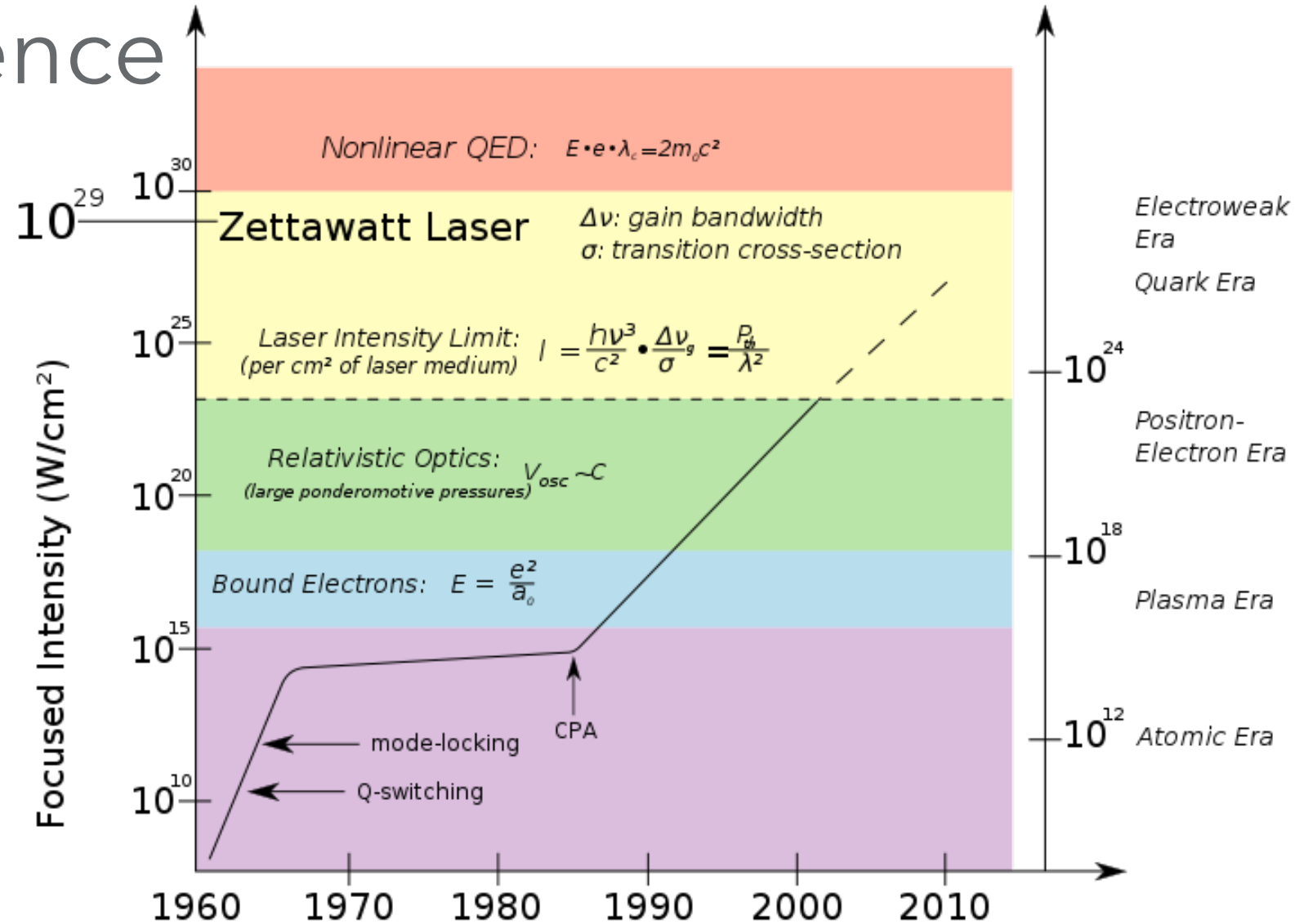
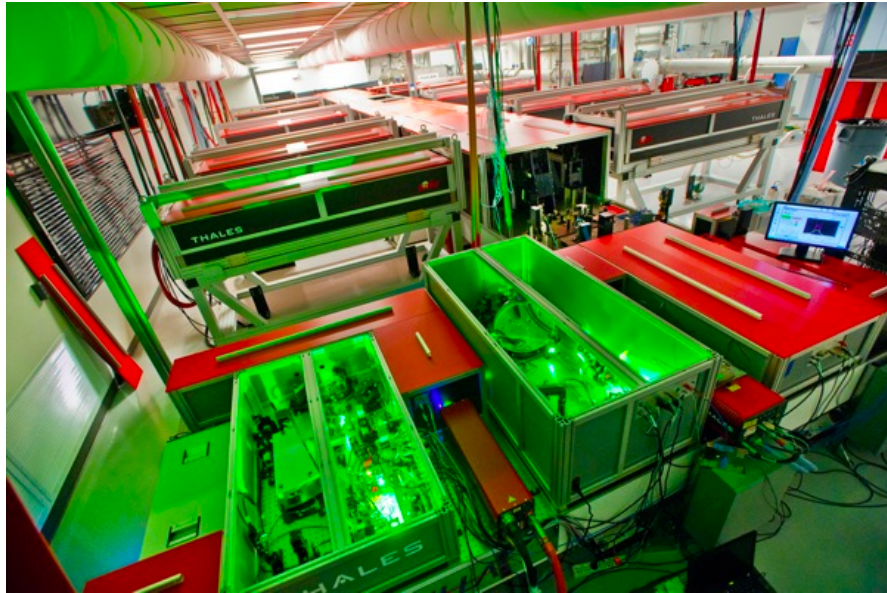


Noble gas jet targets (Strong field HHG)



Polished solid targets (High field HHG)

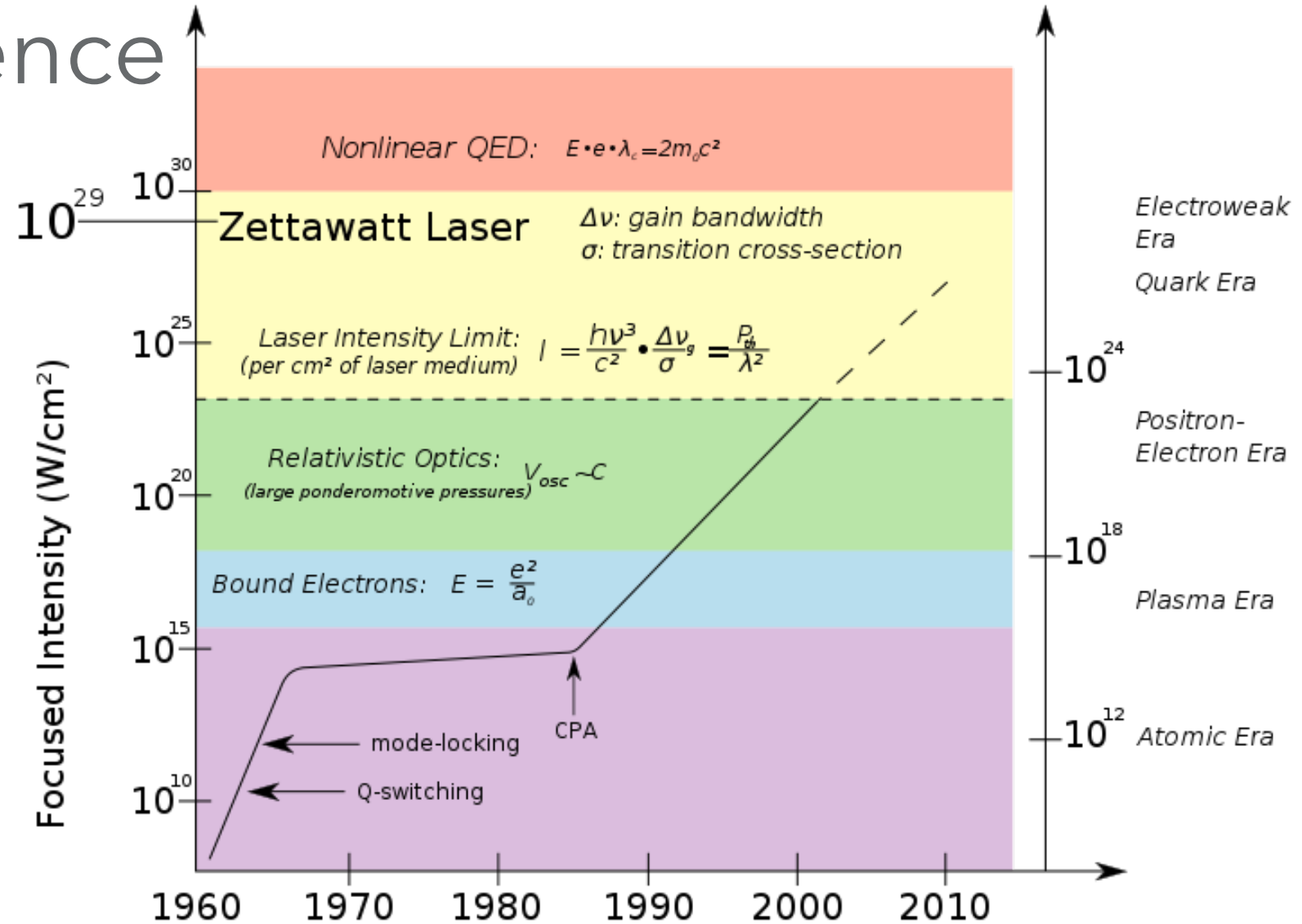
High field science



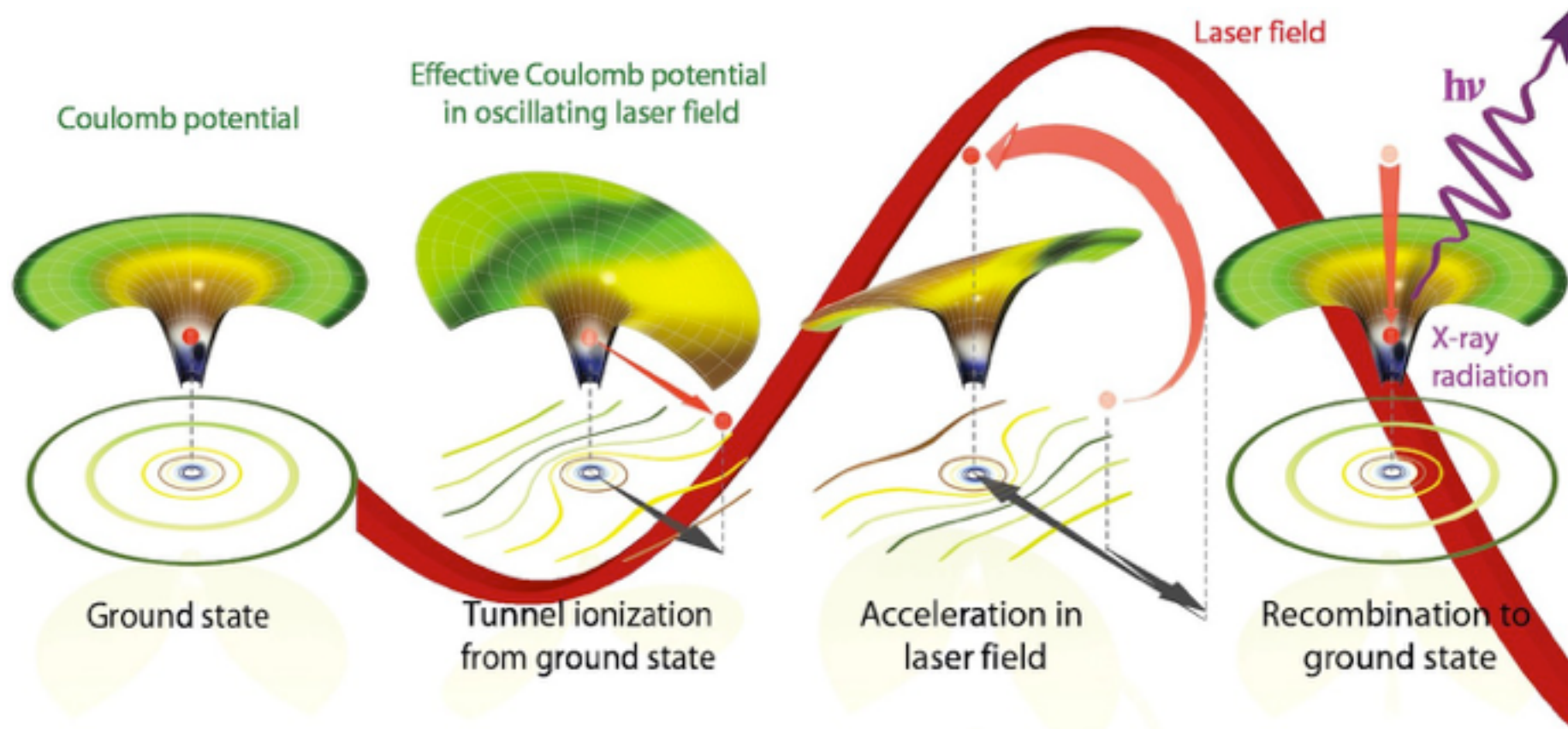
High field science

$$v_q = \frac{e_c E_0}{m_e \omega_0} \sim \lambda \sqrt{I}$$

$$U_p = \frac{1}{2} m_e \langle v_q \rangle^2$$



Single atom HHG



$$E_{\text{cutoff}} = I_p + 3.17 U_p$$

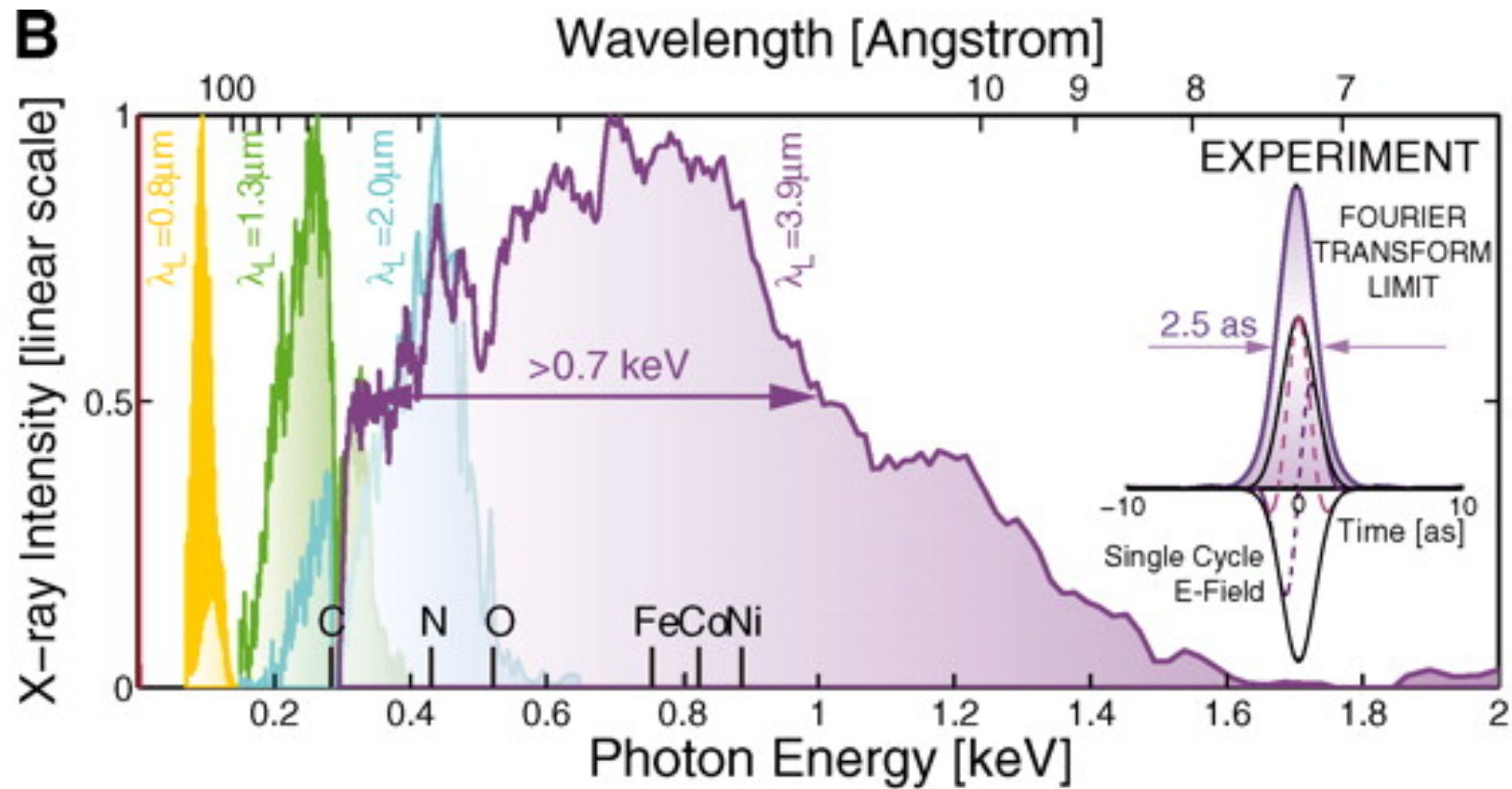
Macroscopic HHG

- Phase matching

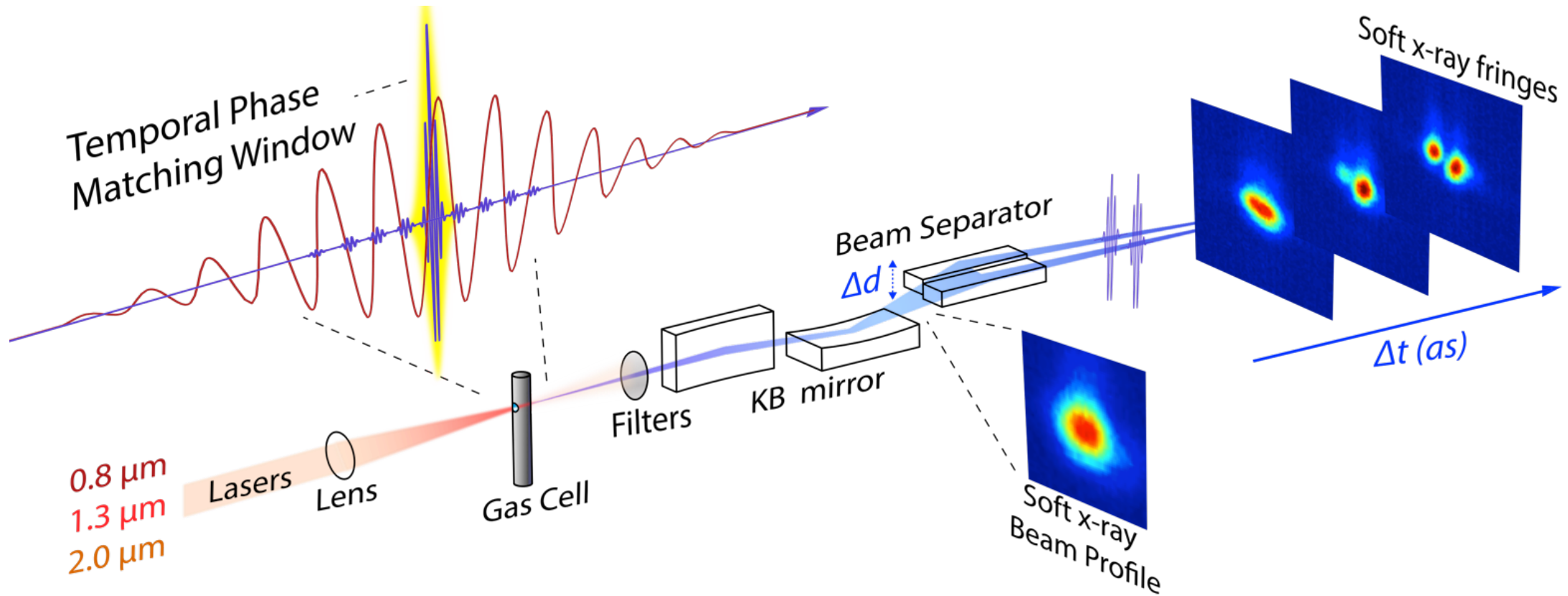


- Fundamental phase affected by
 - Pressure (Neutral gas index of refraction)
 - Ionization fraction (Plasma index of refraction)
 - Focusing (Gouy phase shift)

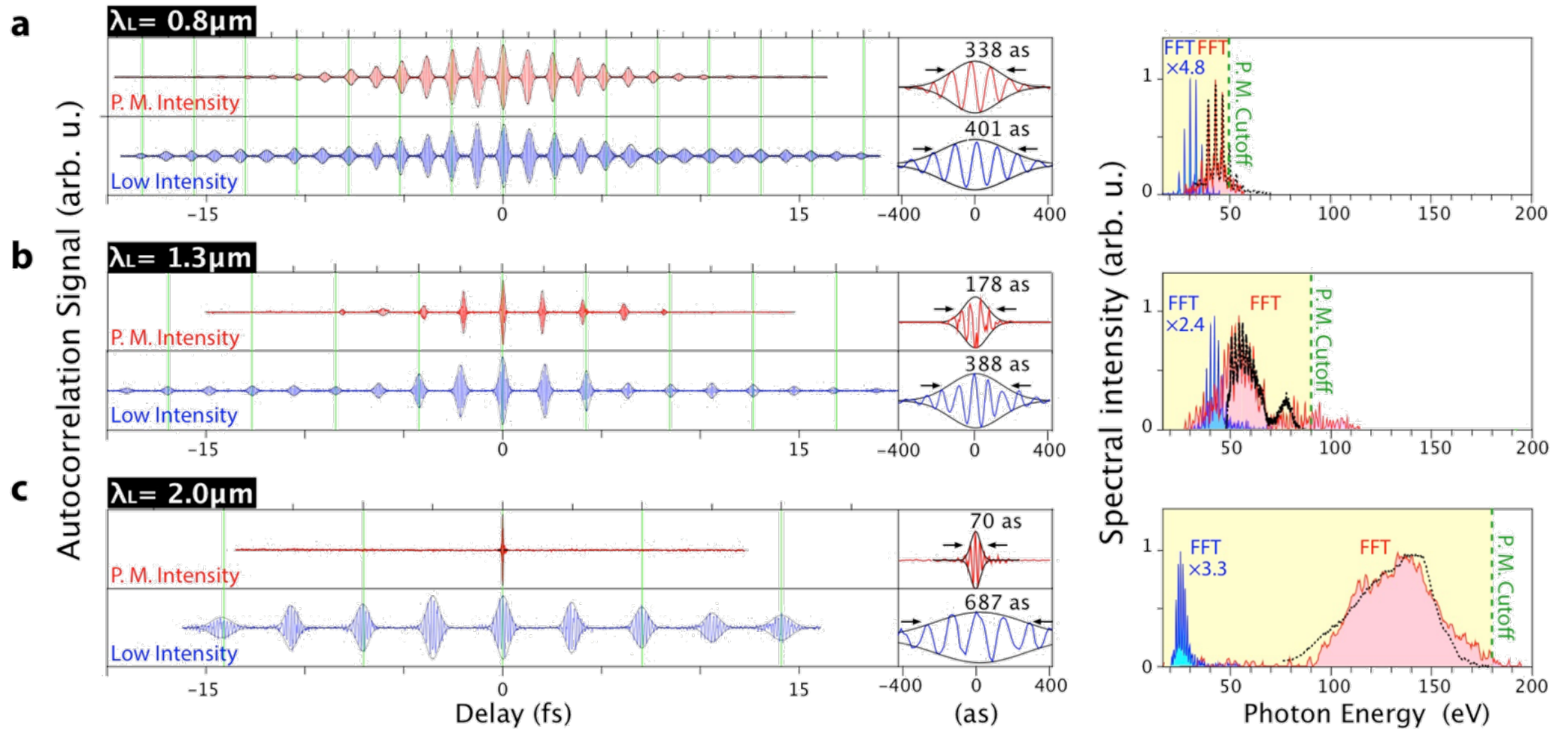
Mid-infrared HHG



X-ray field auto-correlation



Atto-interferograms



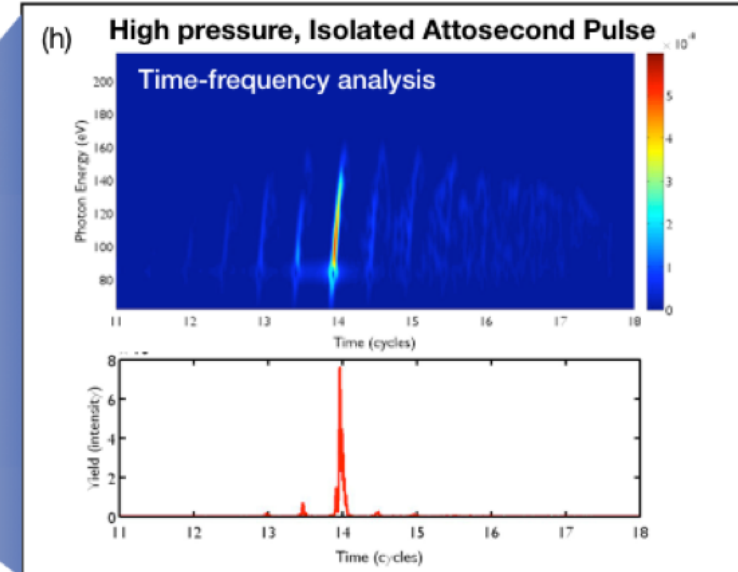
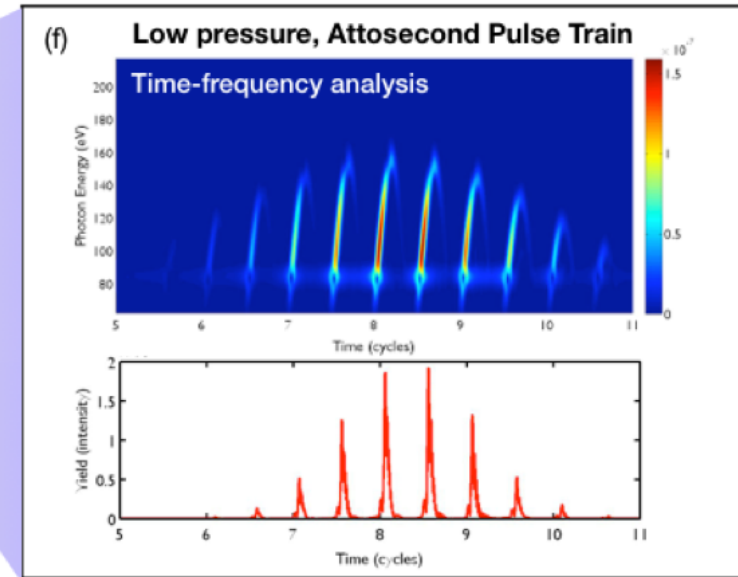
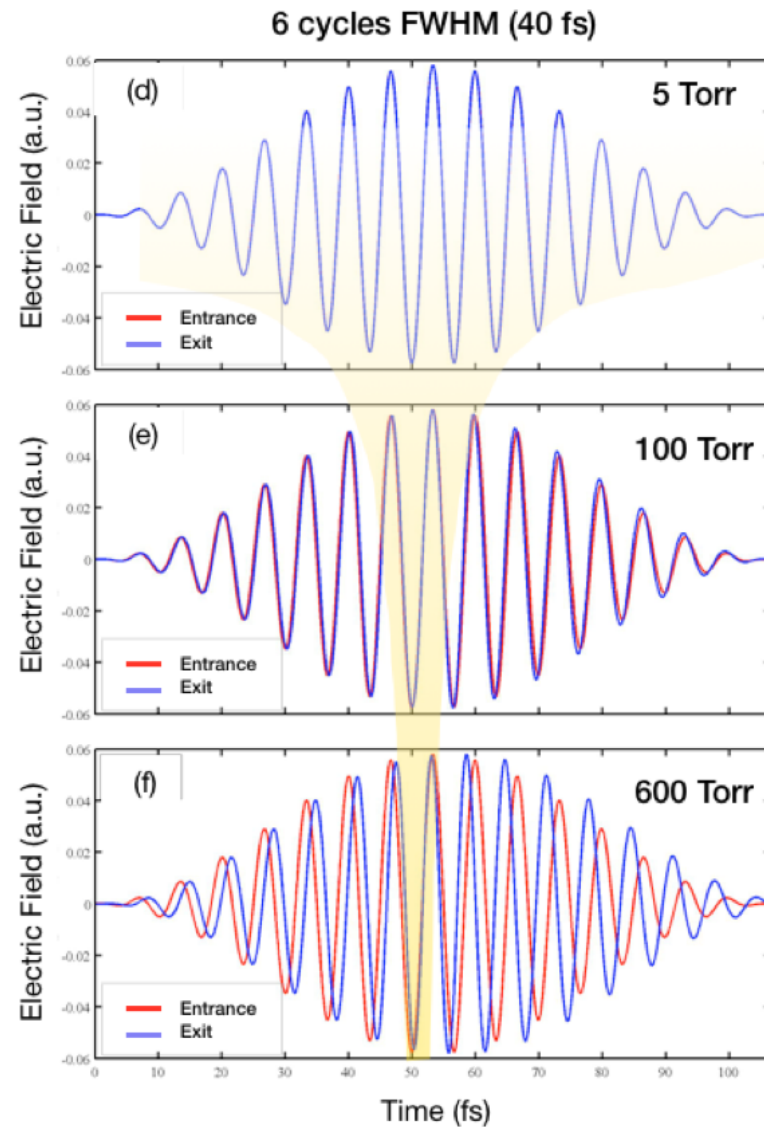
Phase matching window

- Phase matching window shrinks for longer wavelengths

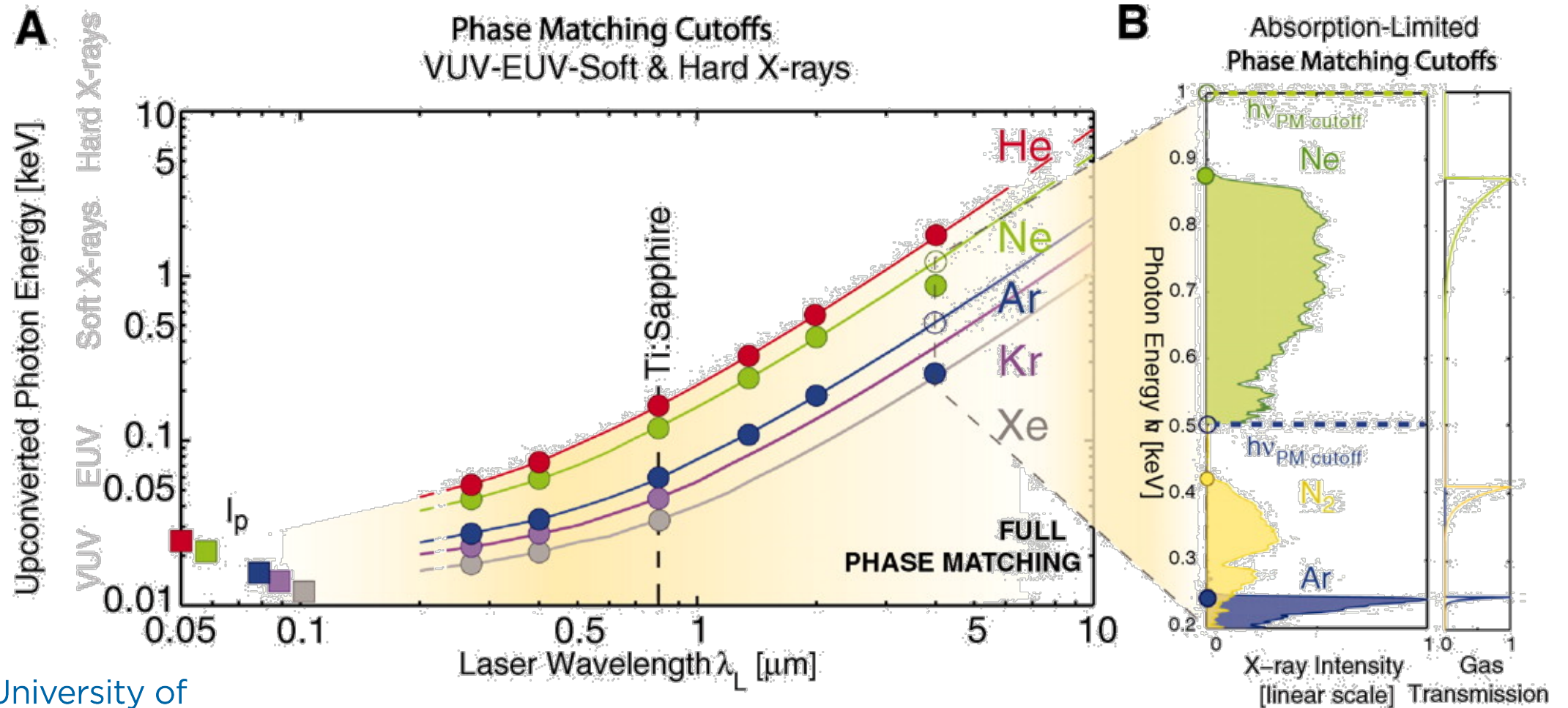
$$\Delta k(t) \approx P \cdot q \cdot \left([1 - \eta(t)] \cdot \delta n \cdot \frac{2\pi}{\lambda_L} - \eta(t) \cdot N_{atm} \cdot r_e \cdot \lambda_L \right)$$

- Shrinkage occurs from
 - Increasing pressure
 - Increasing harmonic order
 - Increasing wavelength
 - Increasing period

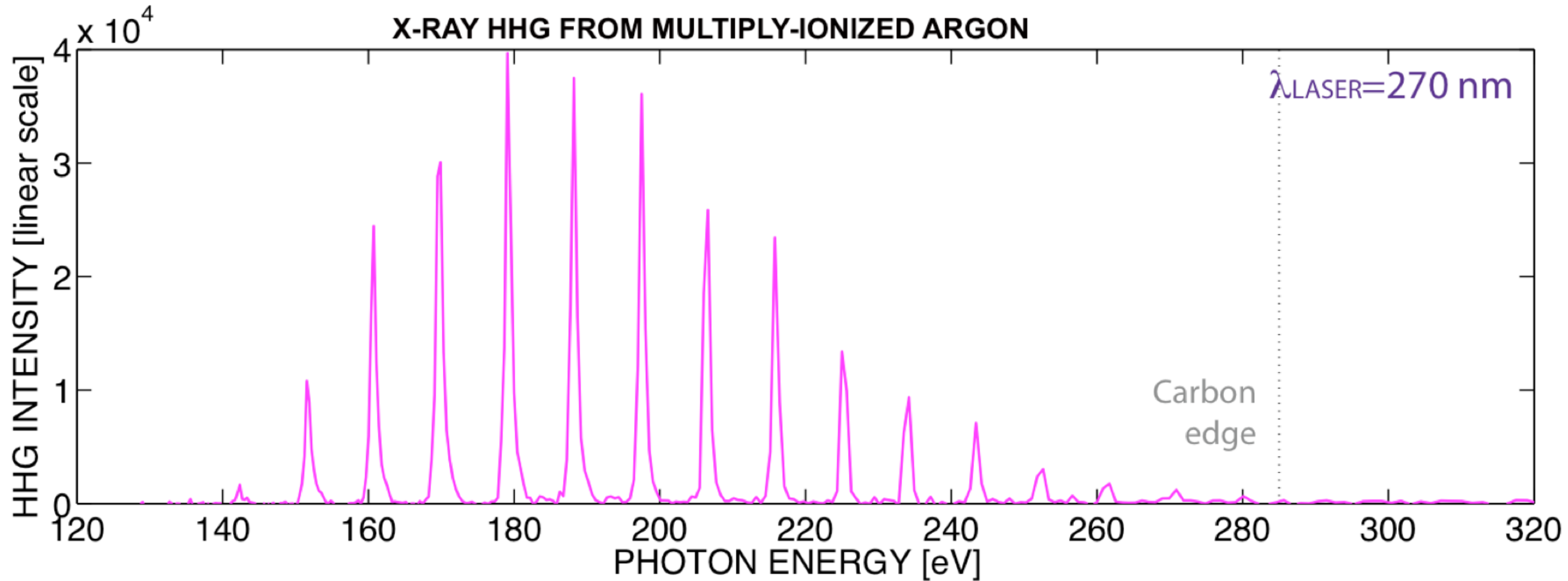
Phase matching



Spectrum of strong field HHG

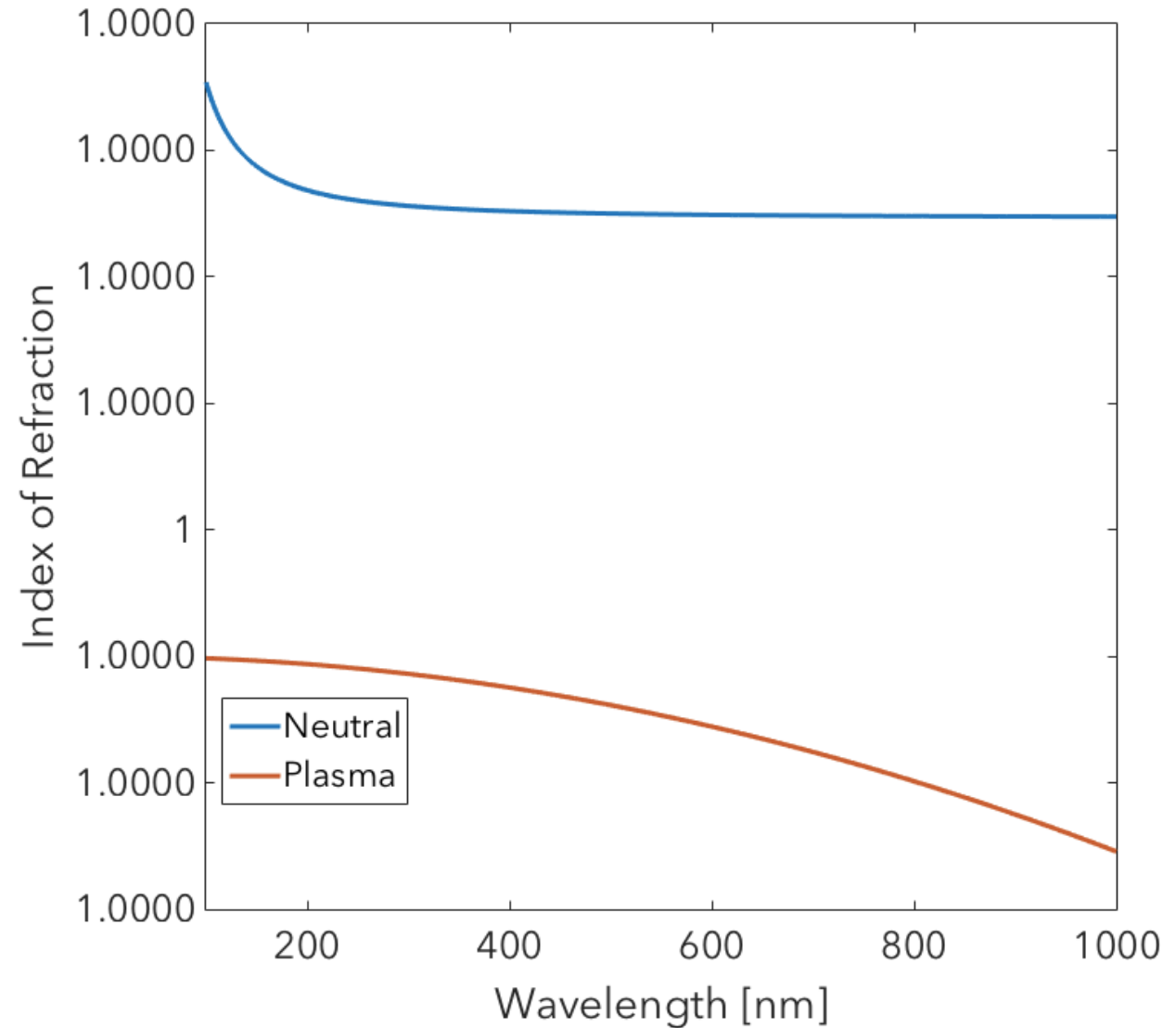


267 nm HHG

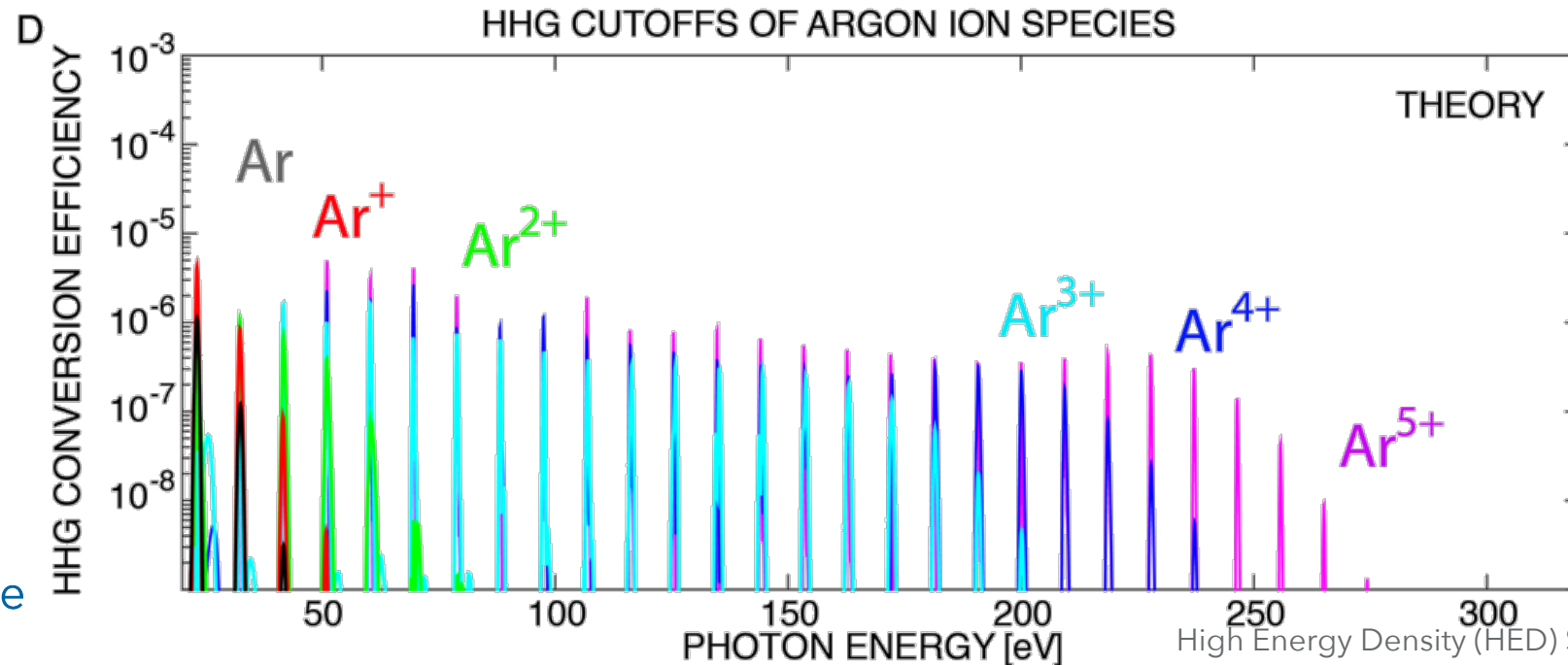
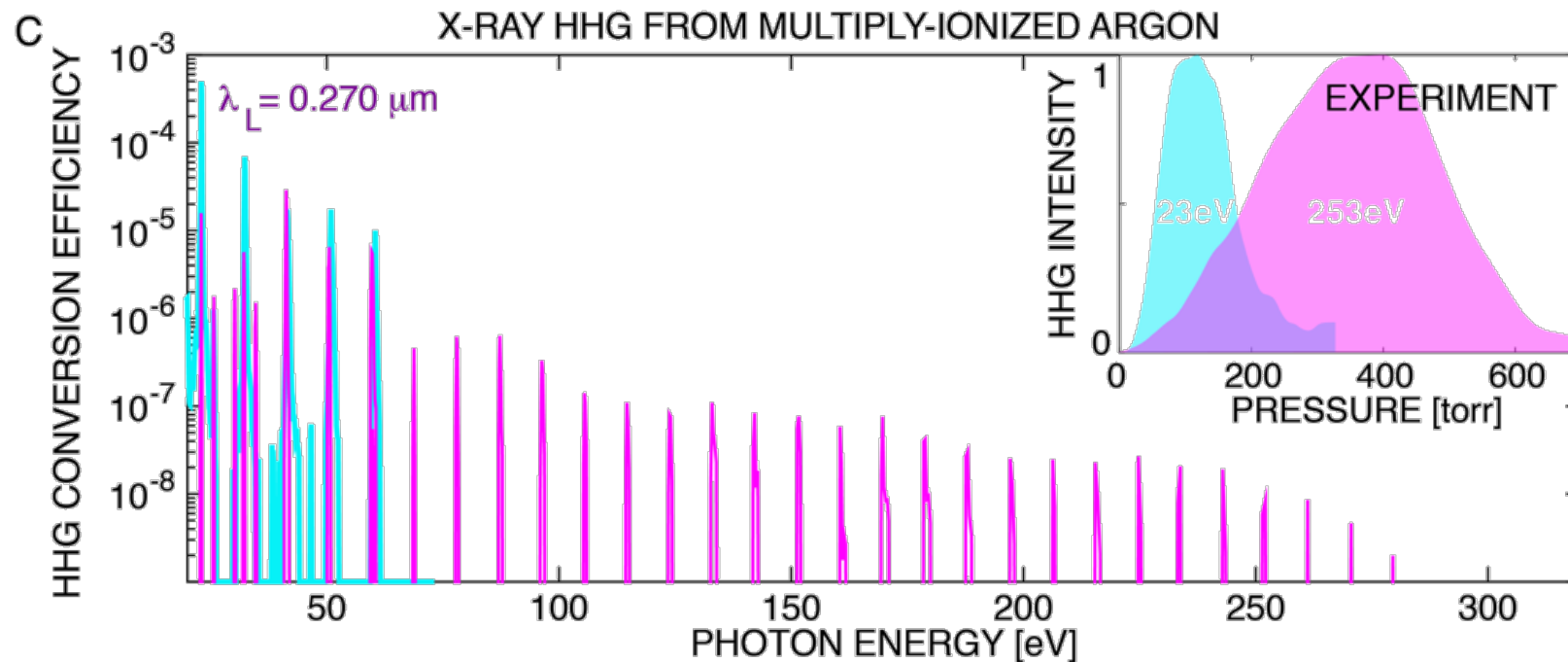


UV Phase matching

- Neutral index of refraction scales inversely with wavelength
- Plasma index of refraction scales with wavelength

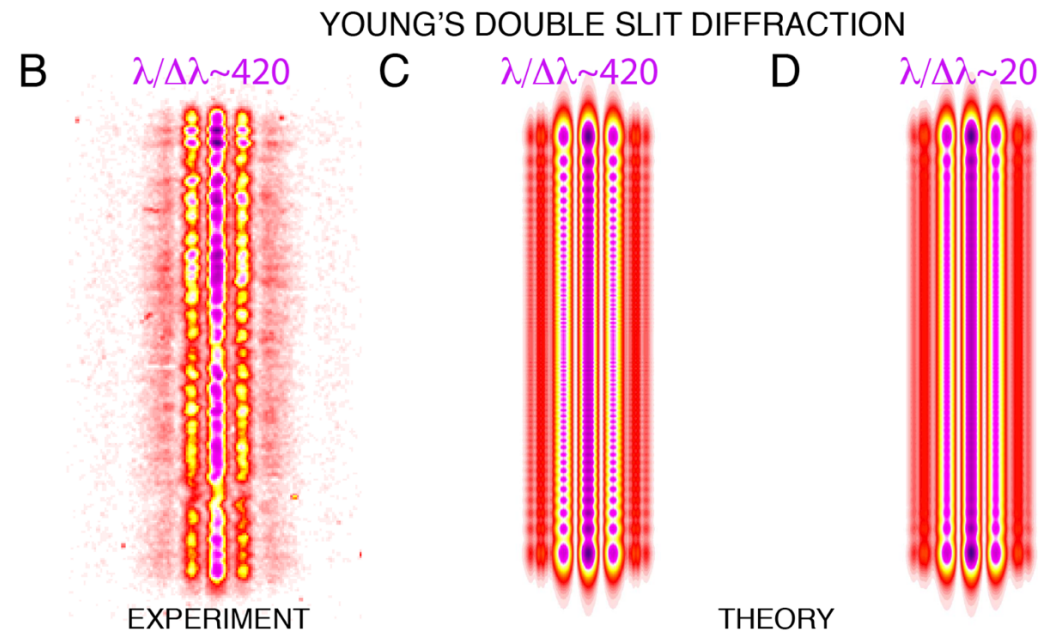
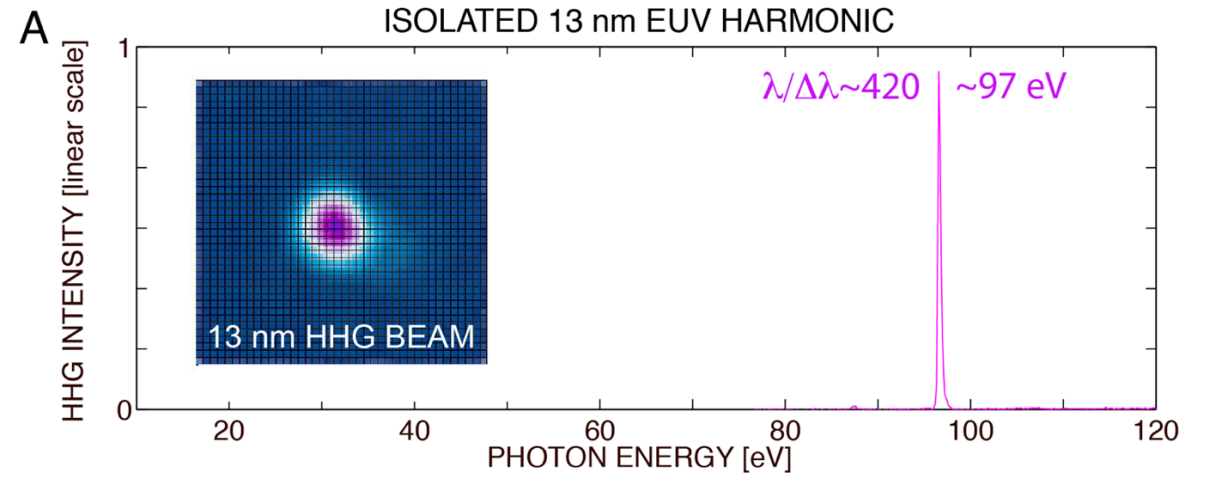


TDSE

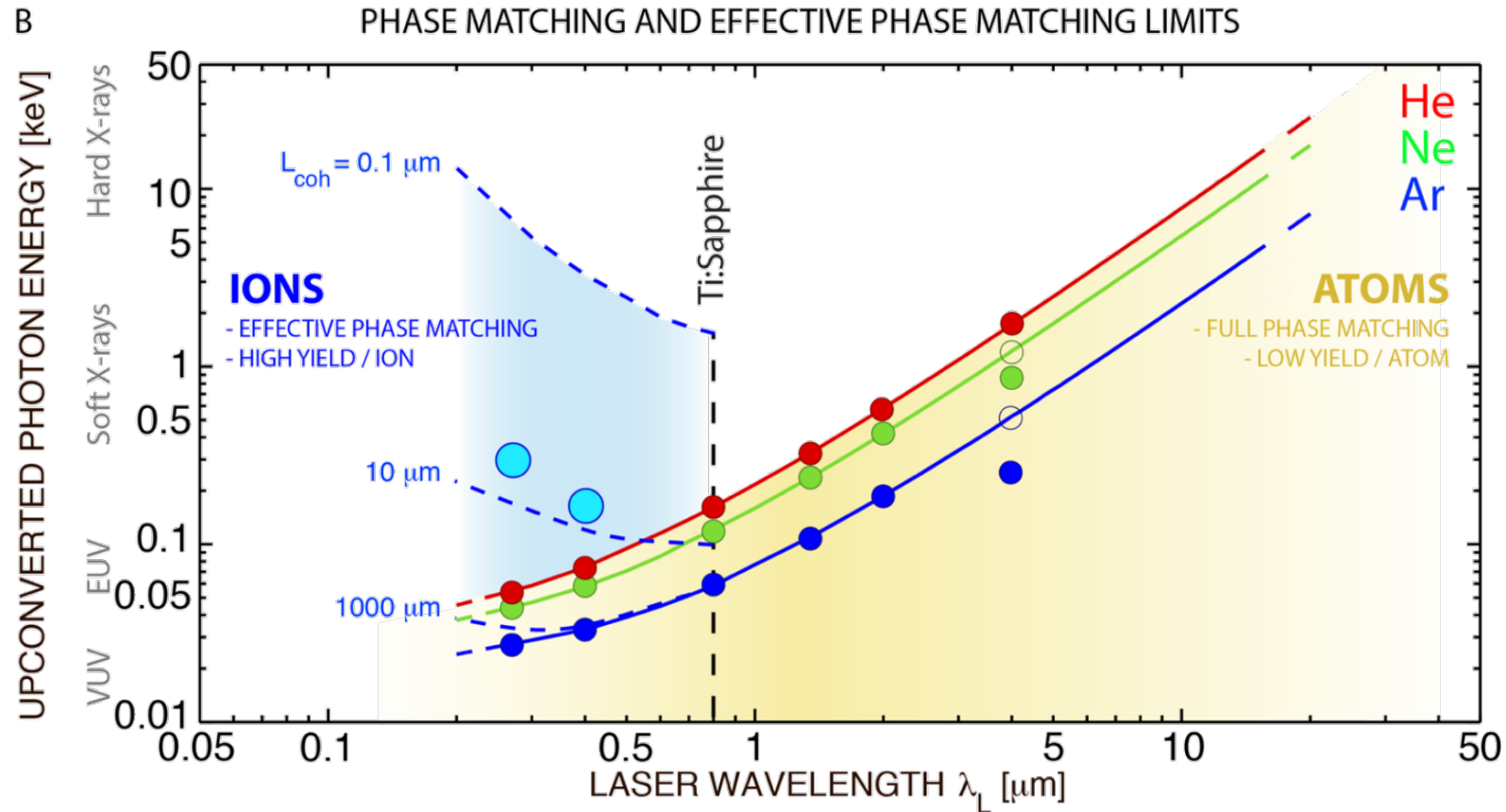


Isolated harmonics

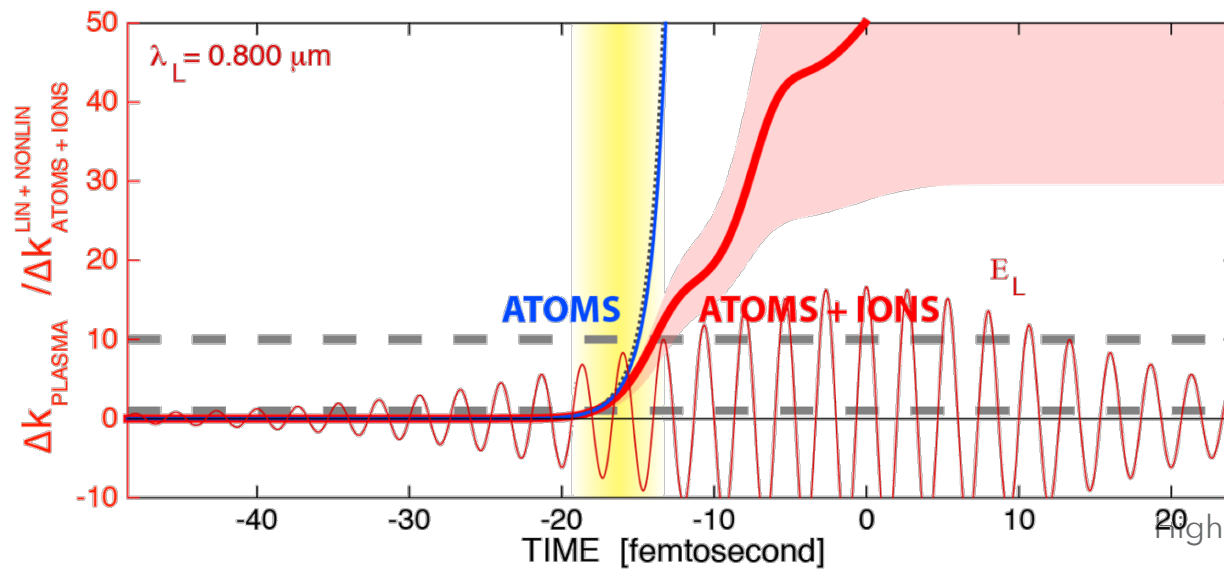
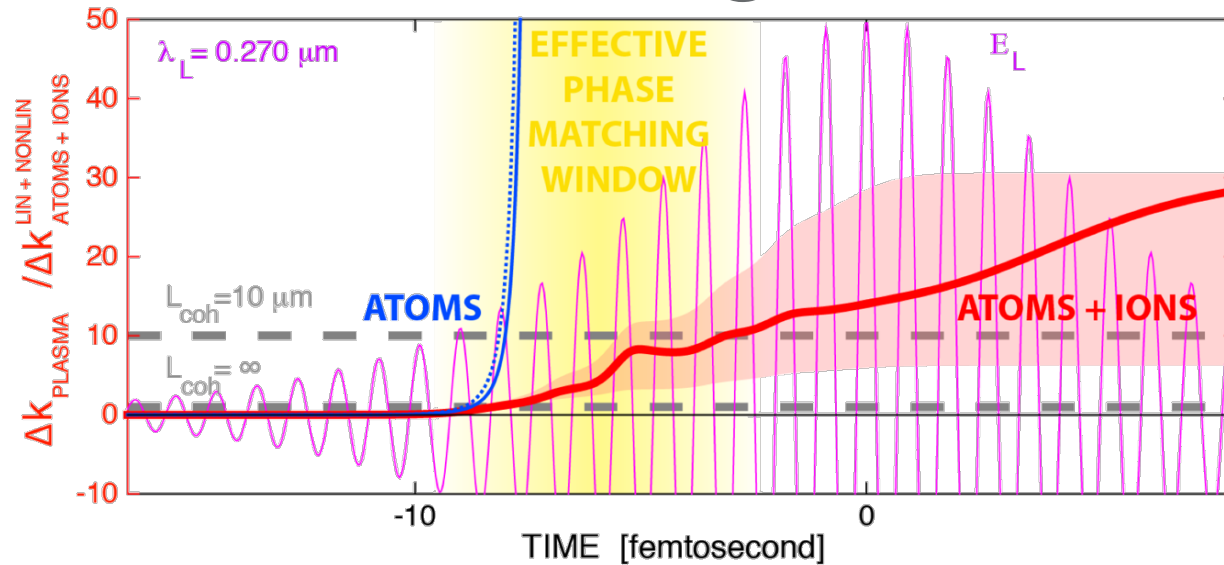
- Notch filters enable spectrally pure wavelengths
- Rh + Be + Si filtering



Full range of wavelength scaling



Larger phase matching window

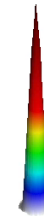
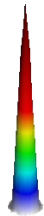


Electron wavefunctions

Linear polarization



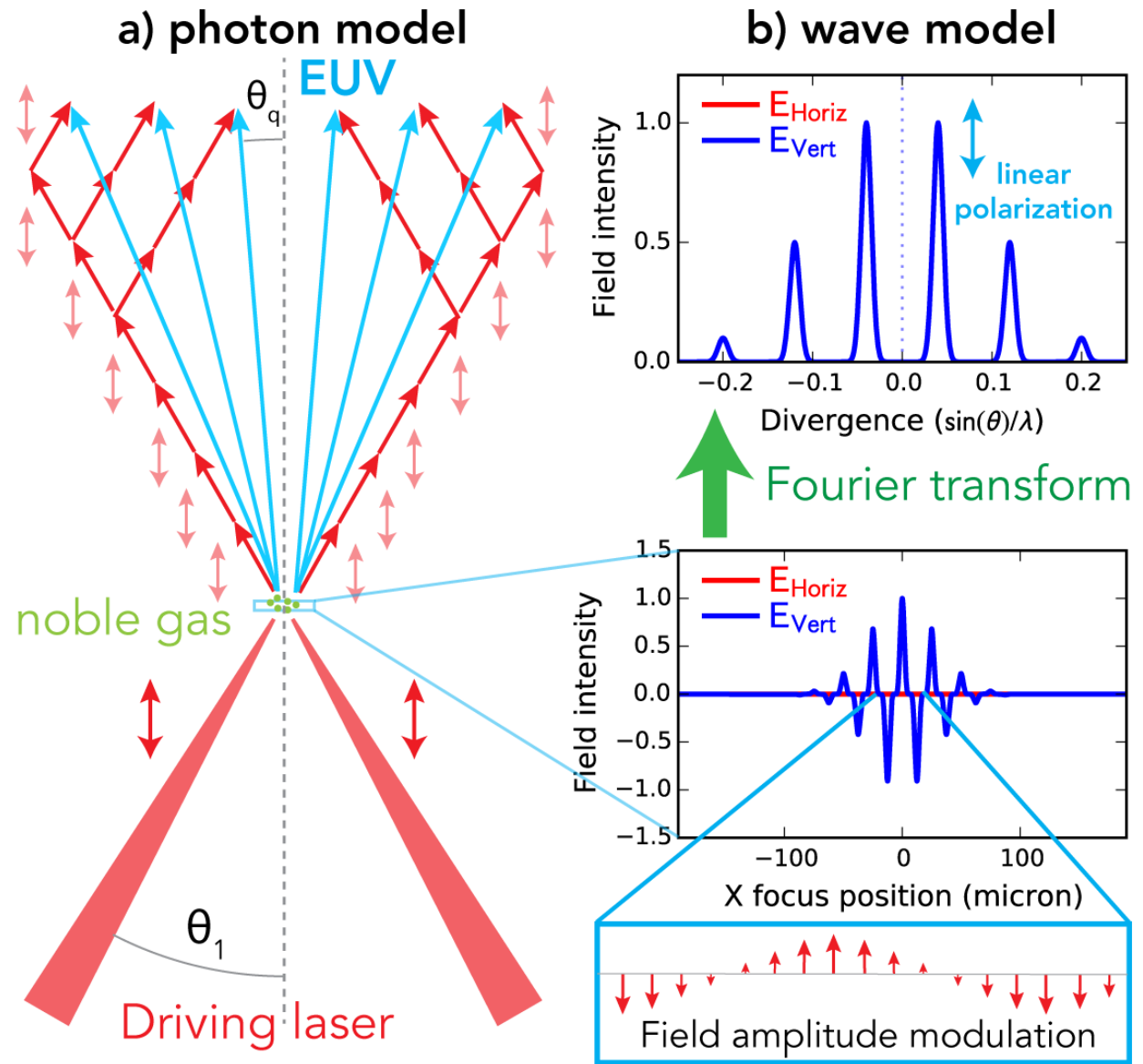
Circular polarization



Non-collinear HHG

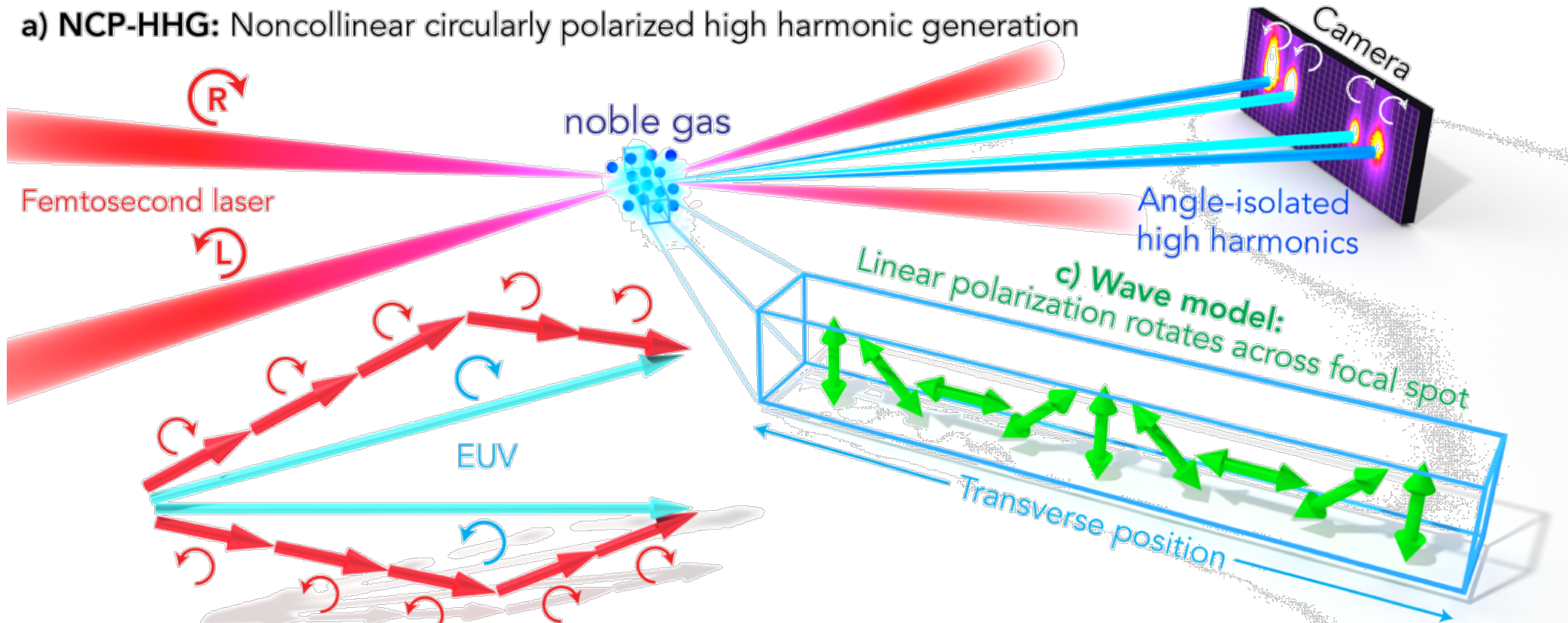
- Conservation of momentum
- Conservation of energy
- Conservation of parity

linear + linear HHG



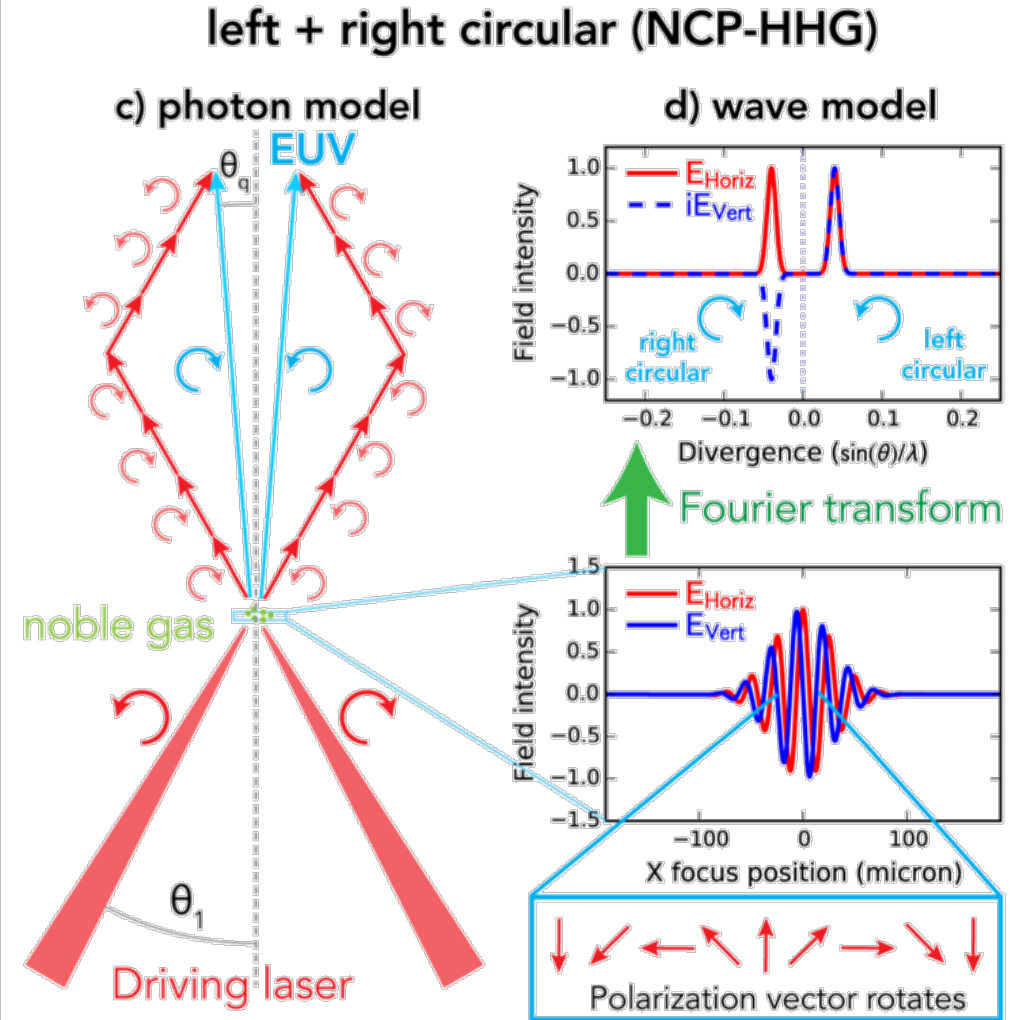
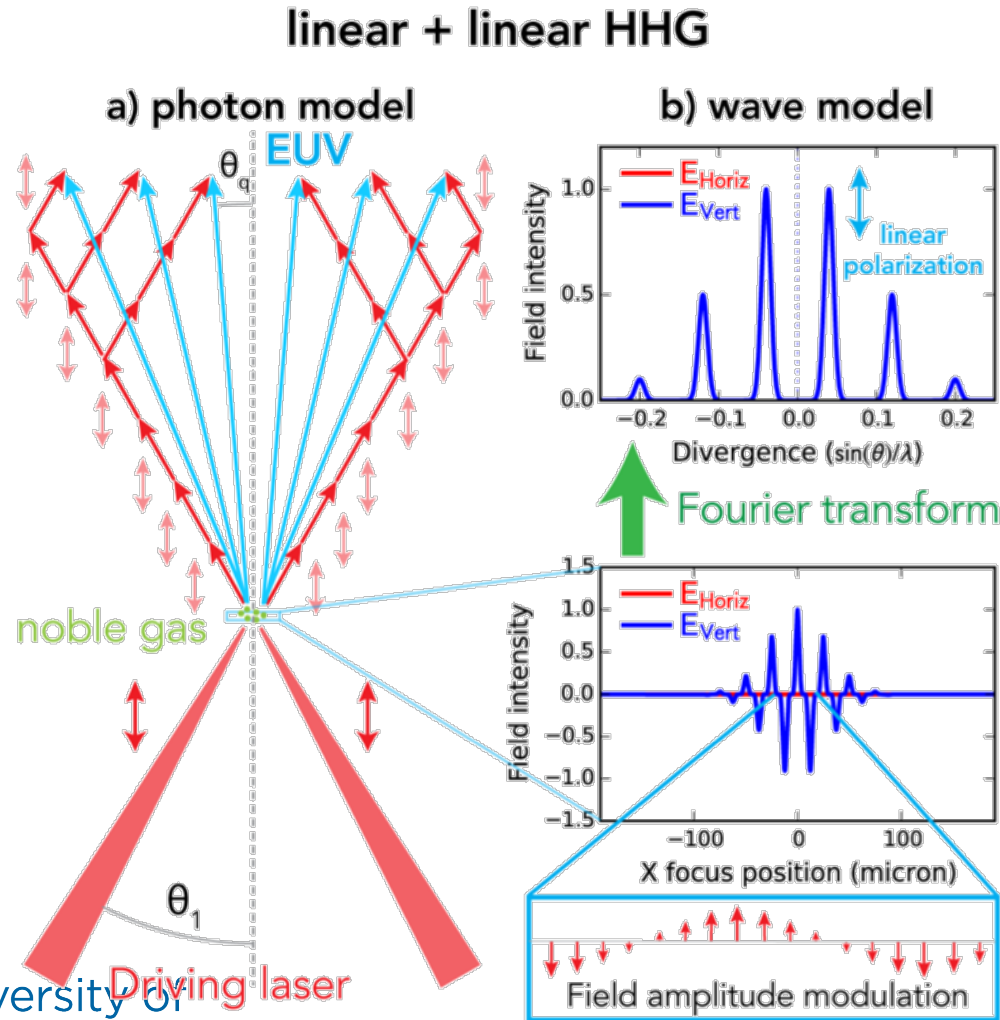
Noncollinear HHG

a) NCP-HHG: Noncollinear circularly polarized high harmonic generation



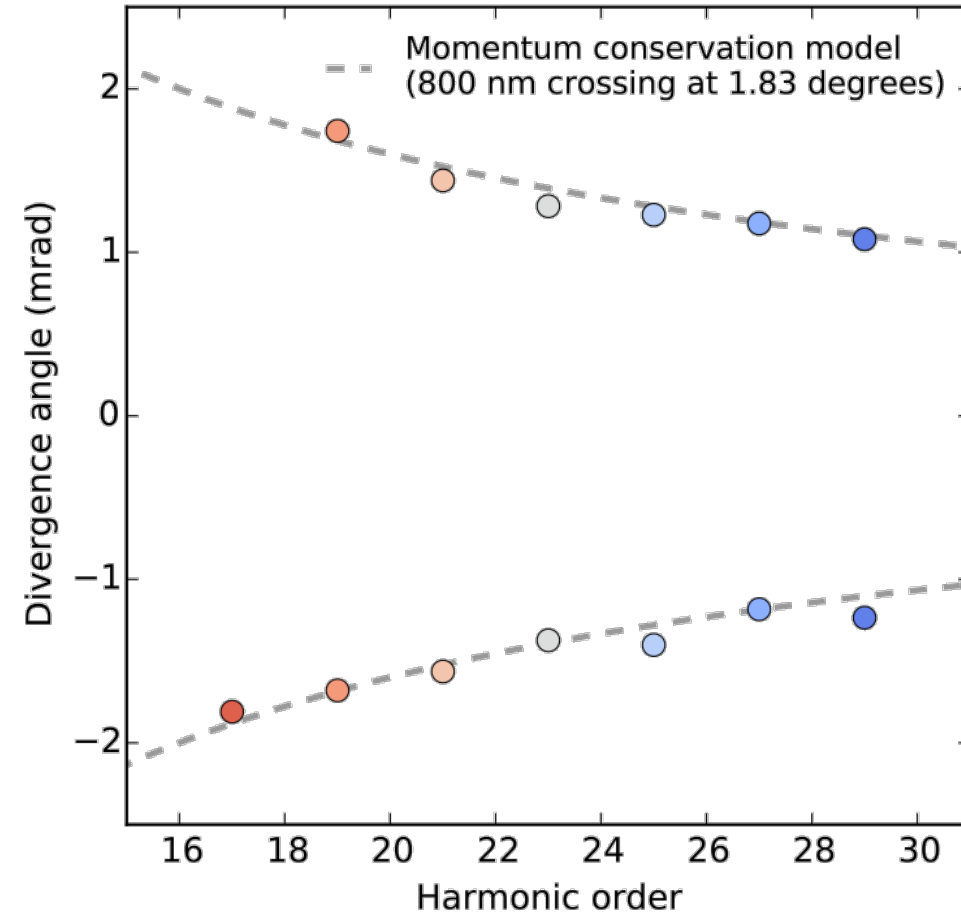
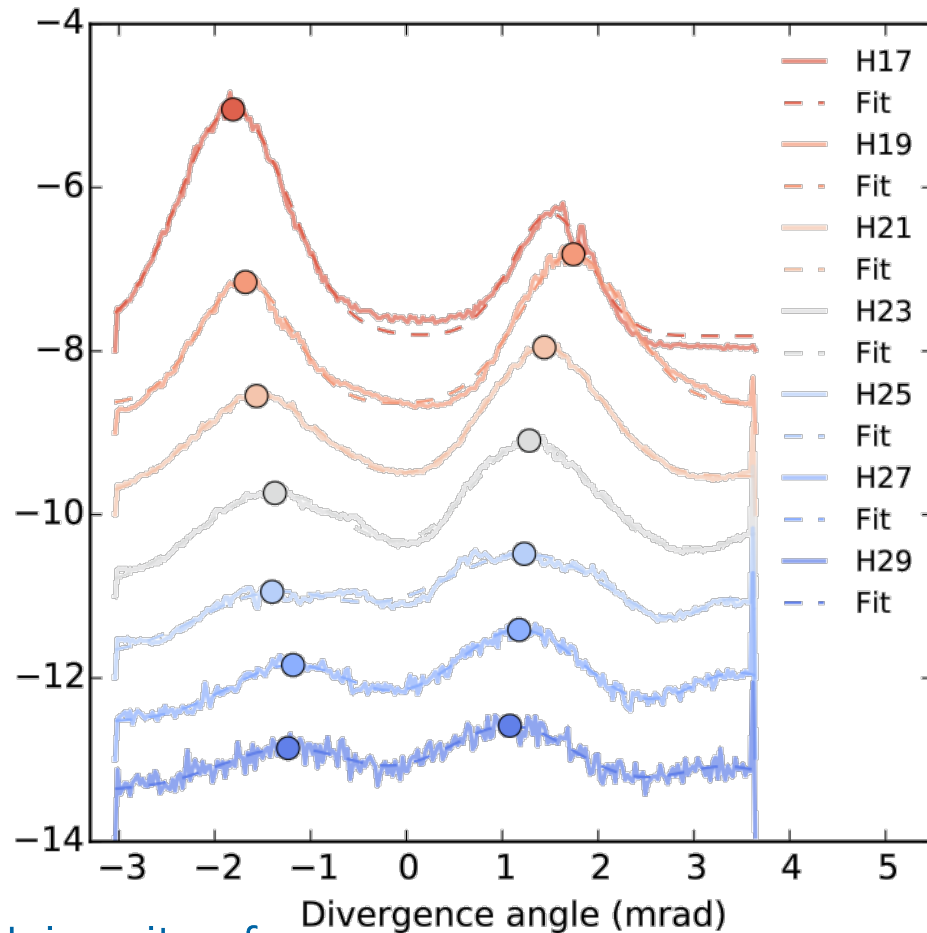
b) Photon model: Addition of photon wave vectors

Conservation of spin angular momentum



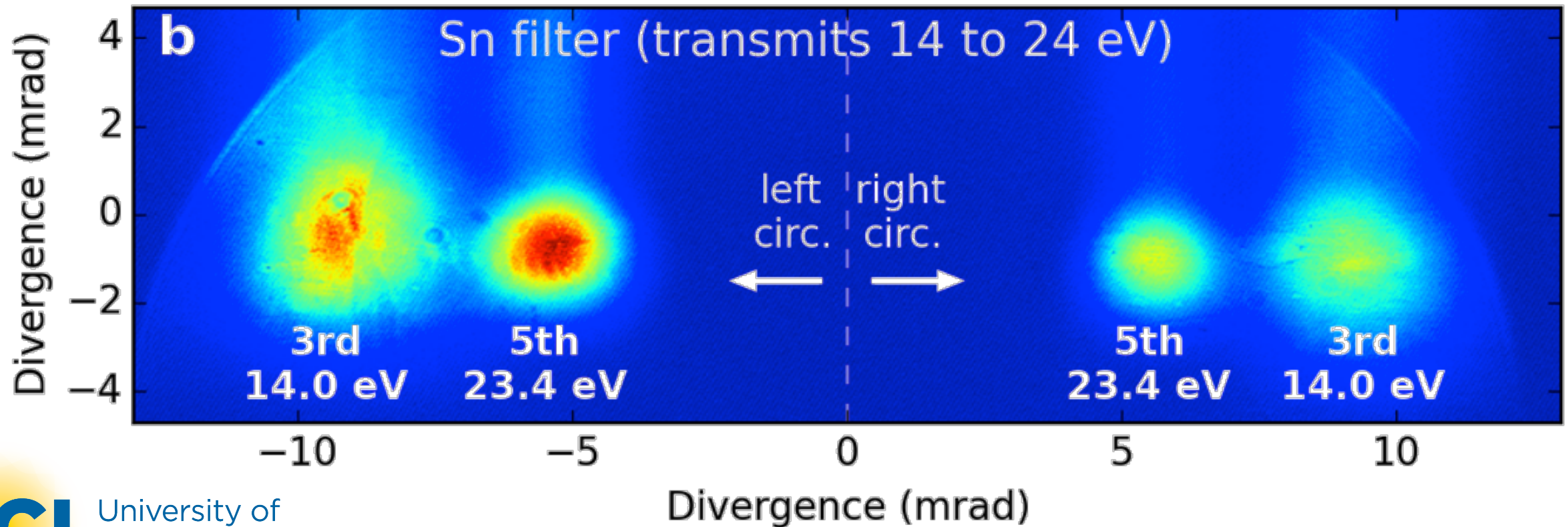
Converging harmonics

Counter-rotating, 150 micron jet



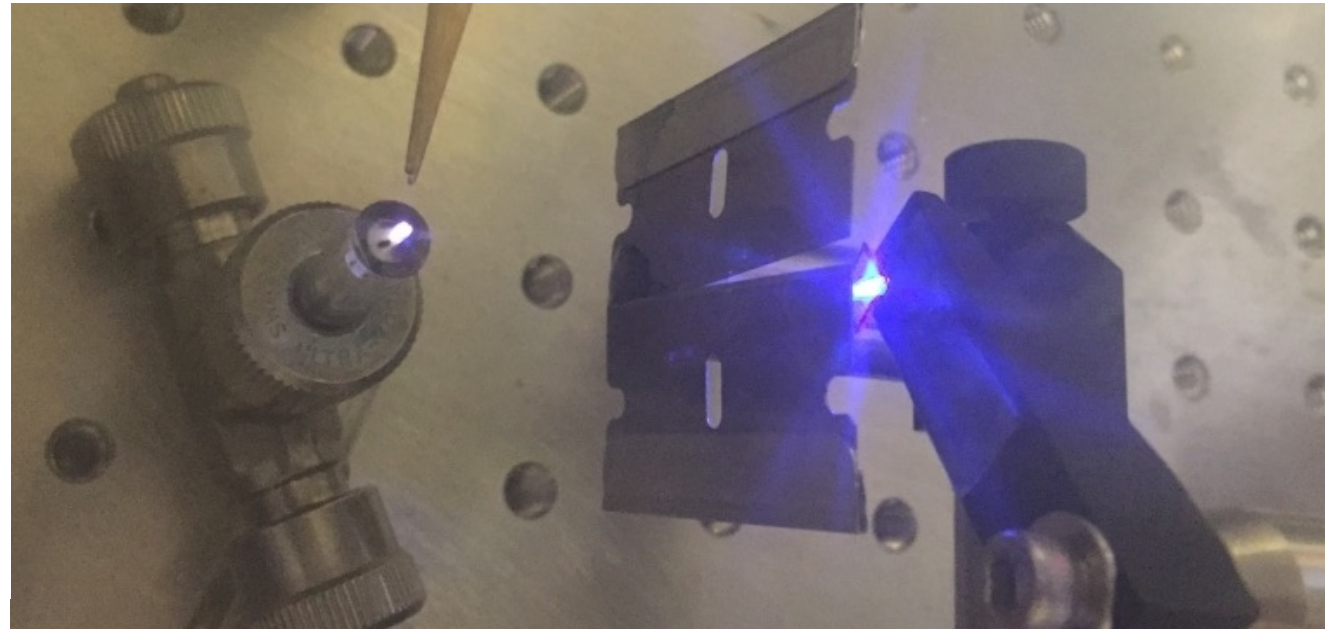
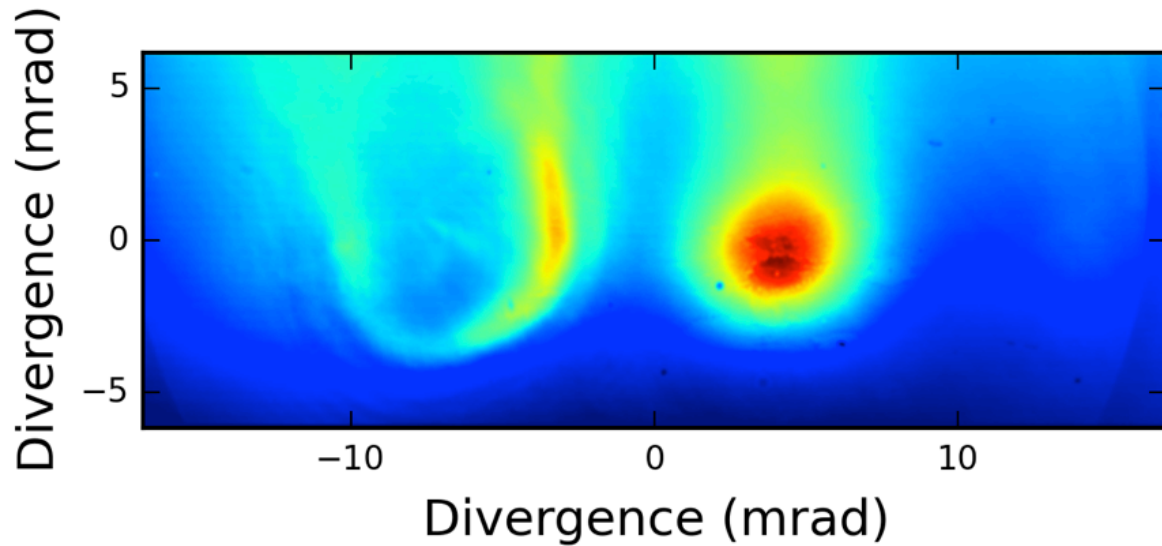
Spatially separated harmonics

- Argon harmonics with 267 nm drivers

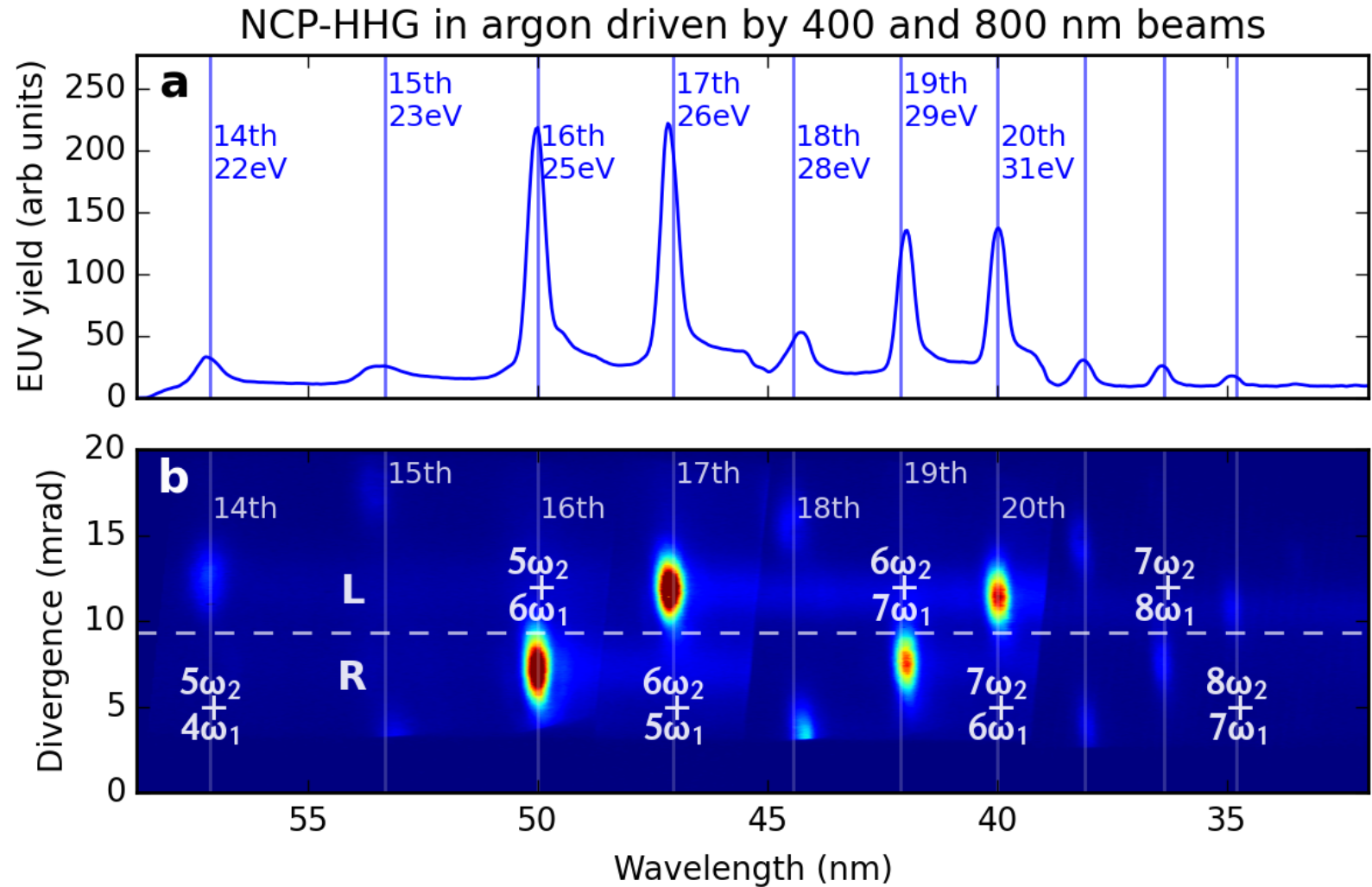
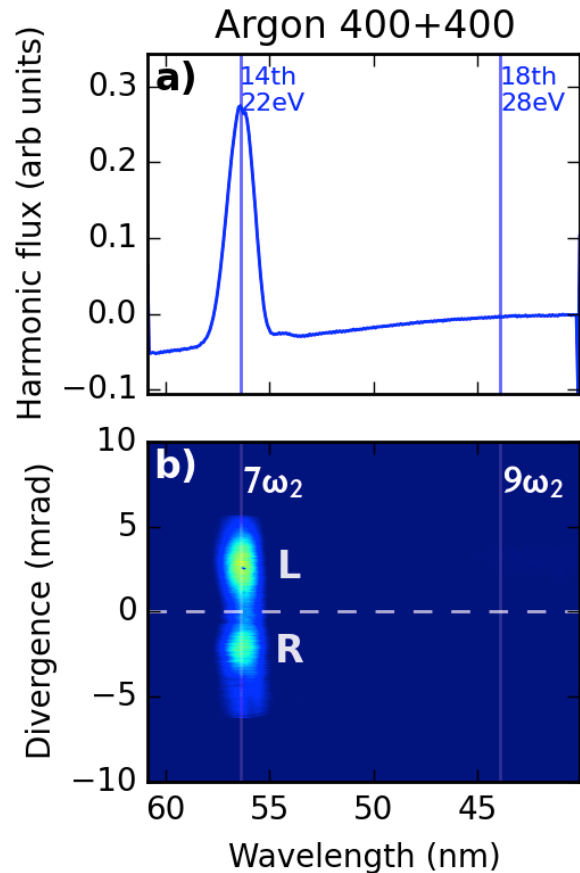


Spatially separated harmonics

- Human hair obstructing harmonic beam but not fundamental

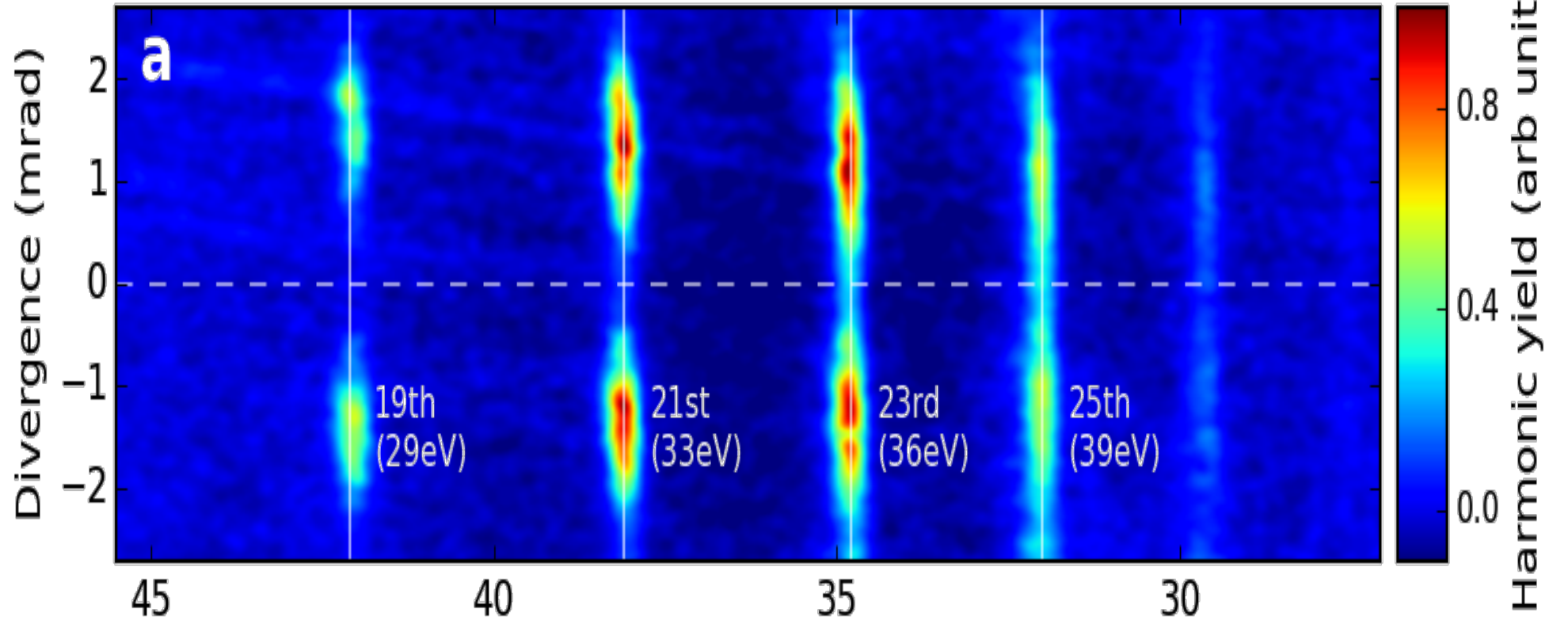


Varying wavelengths

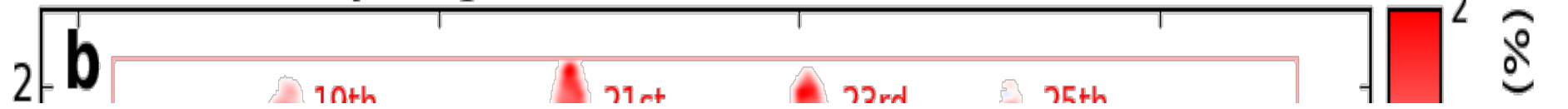


XMCD

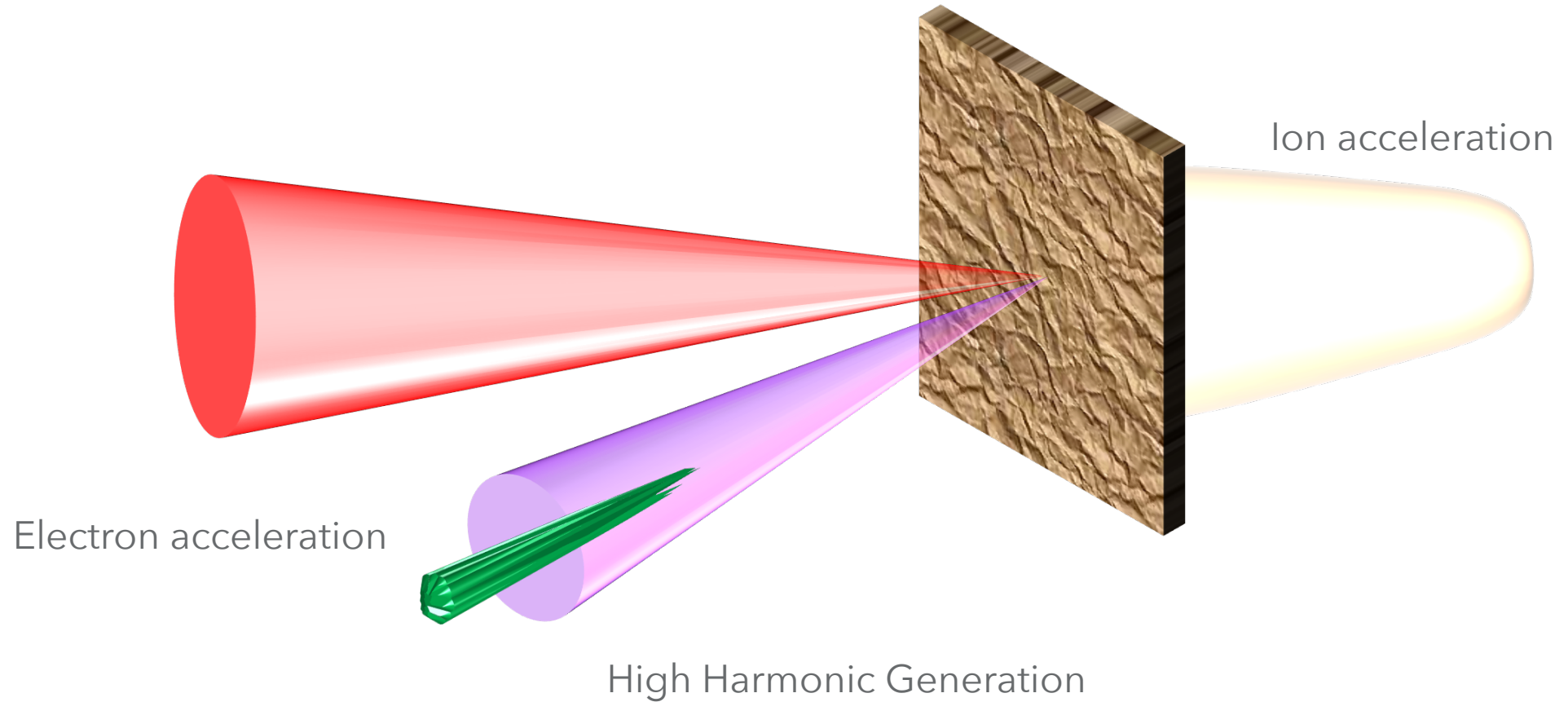
NCP-HHG spectrum through 20 nm iron sample



X-ray magnetic circular dichroism (XMCD)

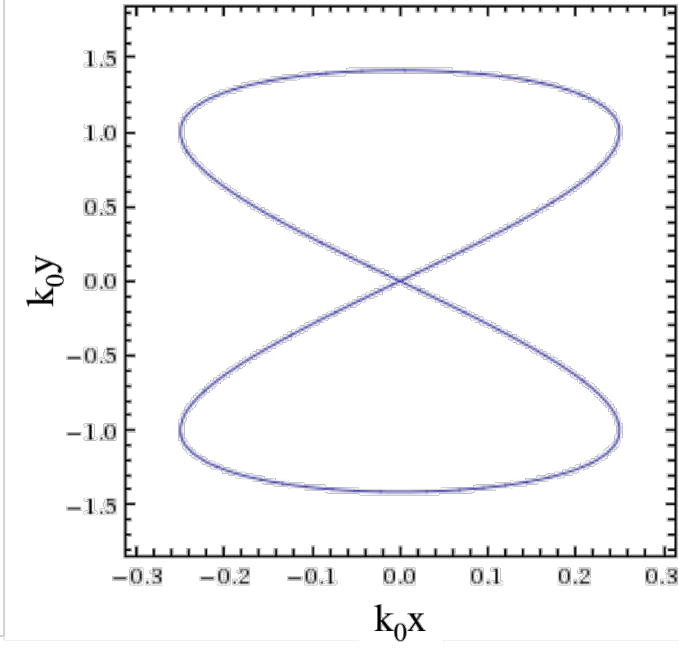
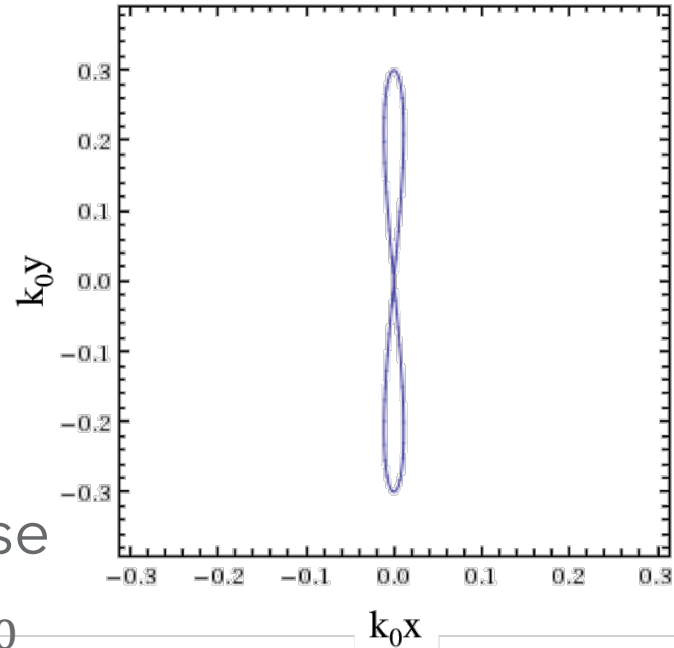


Interactions of lasers and solids



Scaling relationship

- Electron motion described with normalized vector potential
 - Ponderomotive force $\propto \langle a_0 \rangle^2$
 - Lorentz force motion $\propto a_0^2$ in longitudinal, $\propto a_0$ in transverse
 - Relativistic Lorentz factor $\propto a_0$

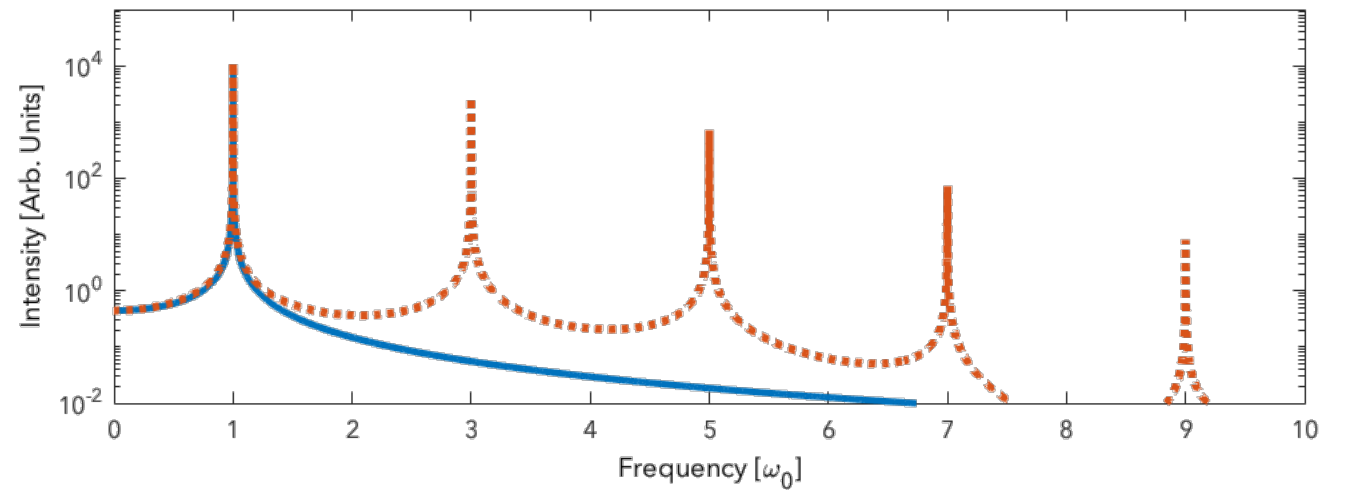
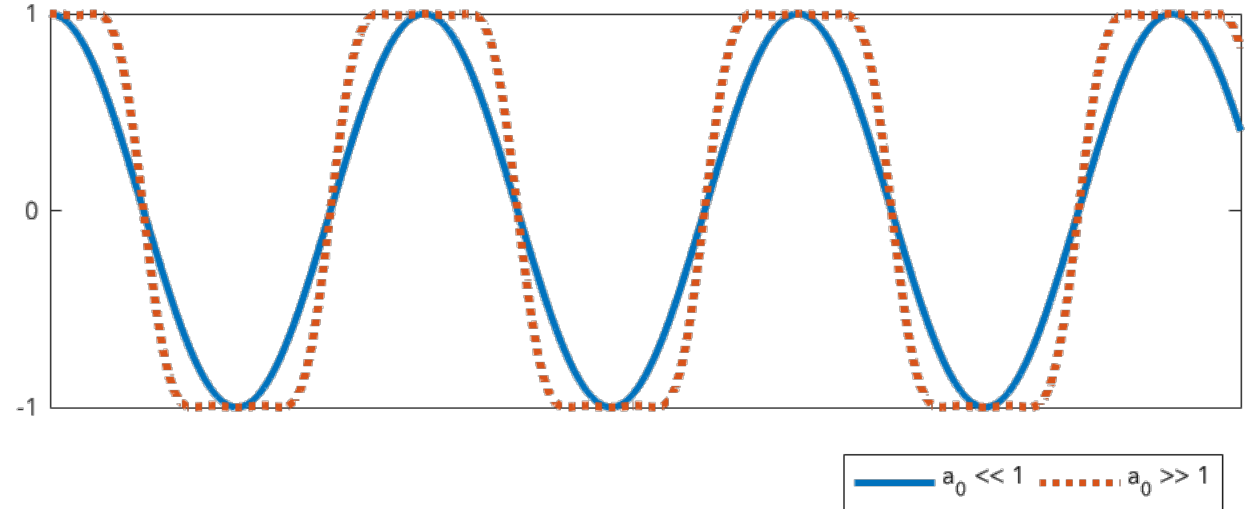


$$a_0 = \frac{p_0}{m_e c} = -\frac{e_c A_0}{m_e c} = -\frac{e_c E_0}{m_e c \omega_0}$$

$$a_0 = 0.85 \times 10^{-9} \lambda \sqrt{I}$$

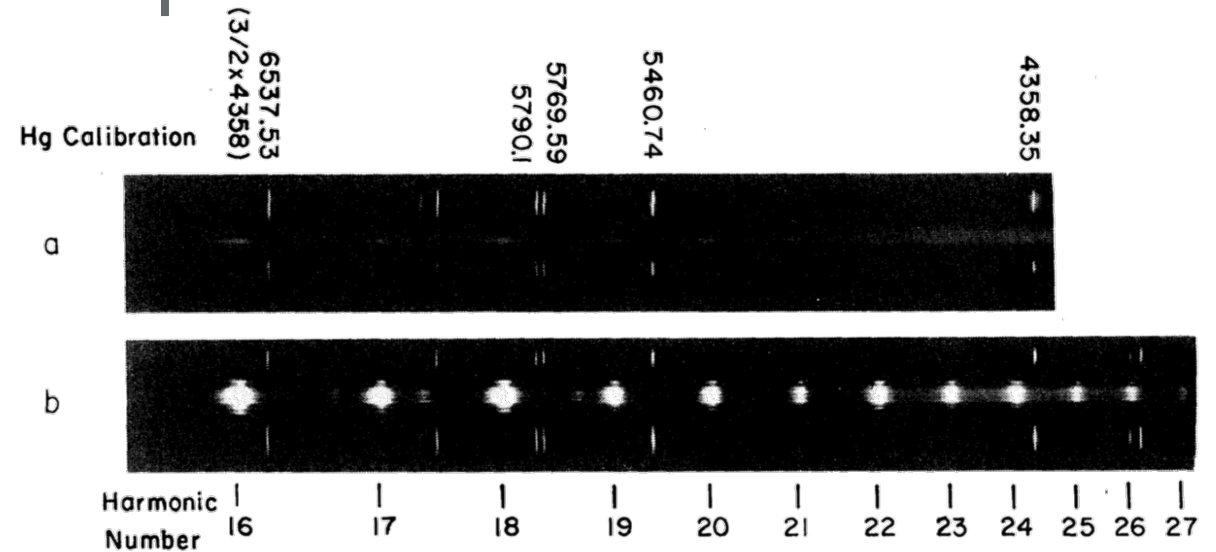
Energy transfer

- Relativistic HHG from aharmonic motion
- HHG from solids is a bulk phenomena
- Relativistic oscillating mirror model



Early relativistic HHG experiments

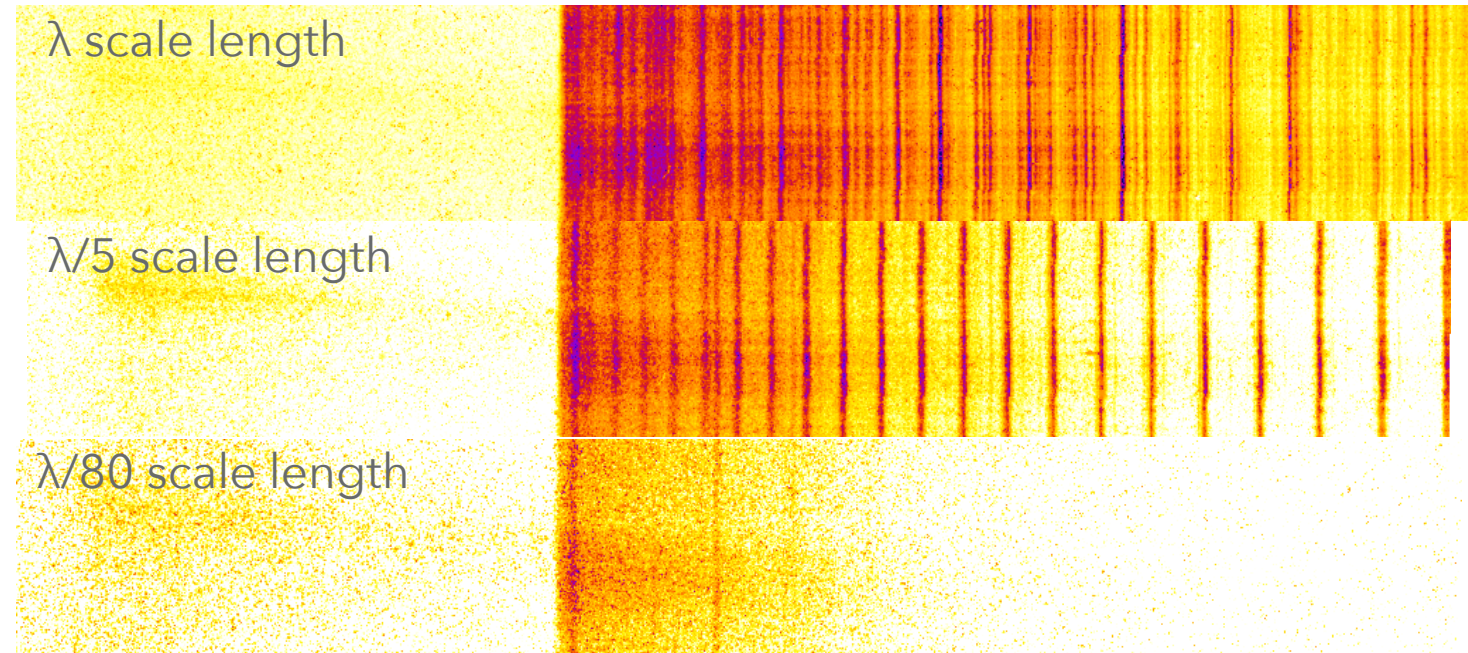
- 1981 CO₂ laser experiment
 - 10^{16} Wcm⁻² on target
 - 8 beams ~1 kJ
 - 0.6 ns FWHM envelope
- Since CPA all experiments at NIR
- Evidence of $I\lambda^2$ scaling



H. L. Carman, D. W. Forslund, and J. M. Kindel, PRL **46**, 29 (1981)

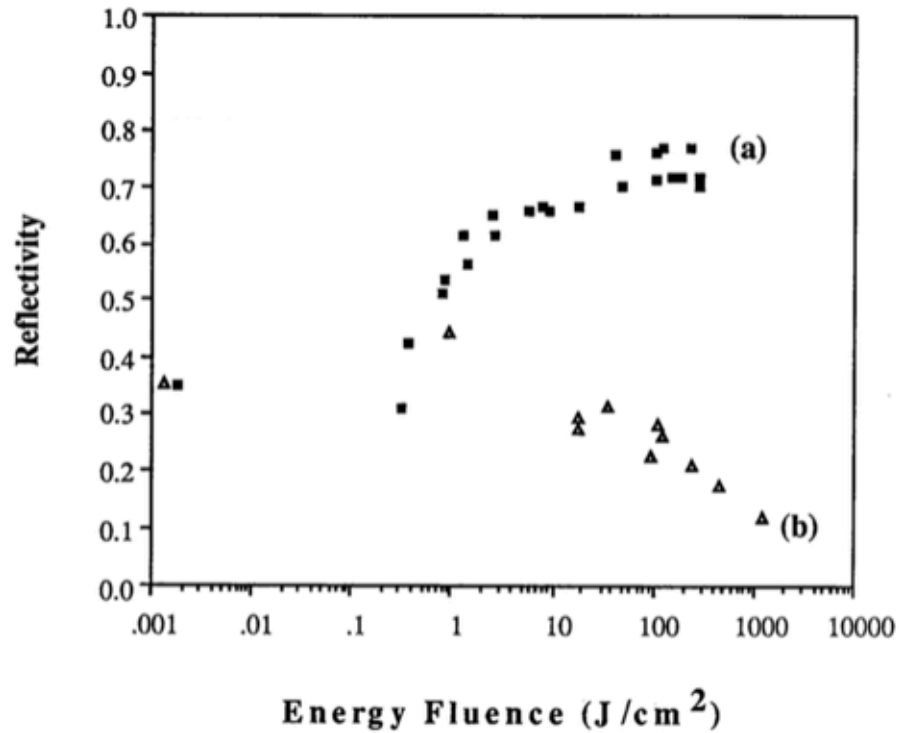
Scale length influence on HHG

- 800 nm experiments
- $10^{17} - 10^{21} \text{ Wcm}^{-2}$
- Preplasma controlled with heating beam

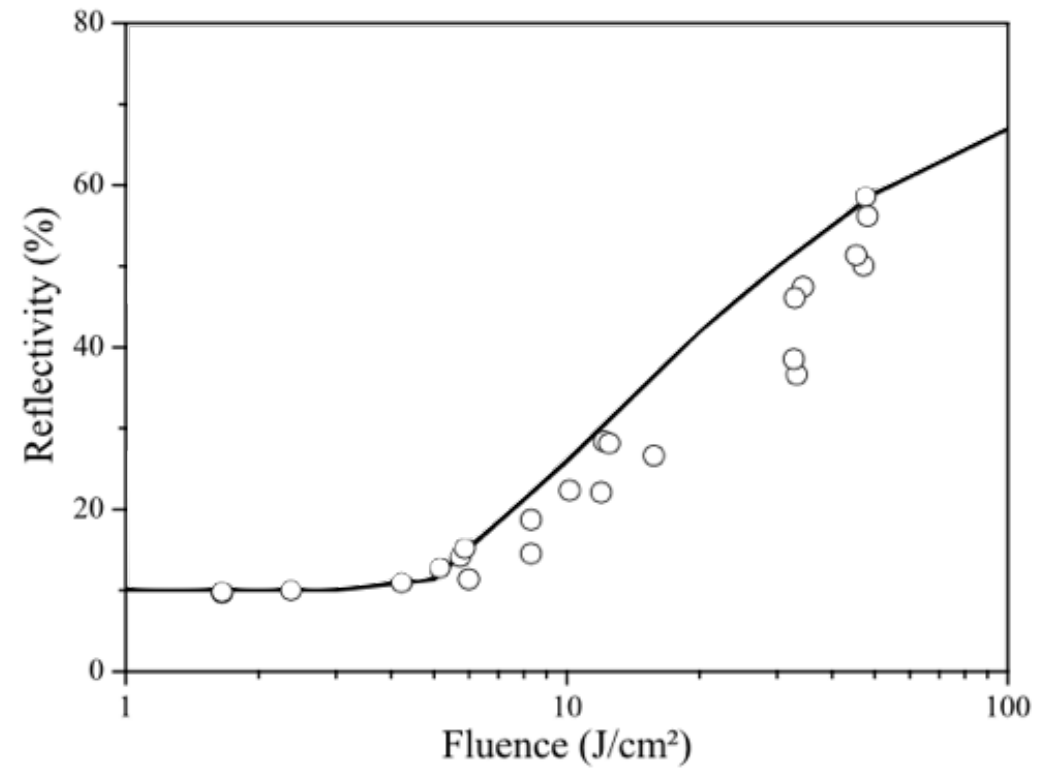


F. Dollar, et al., PRL **110**, 175002 (2013)

Laser absorption into solids



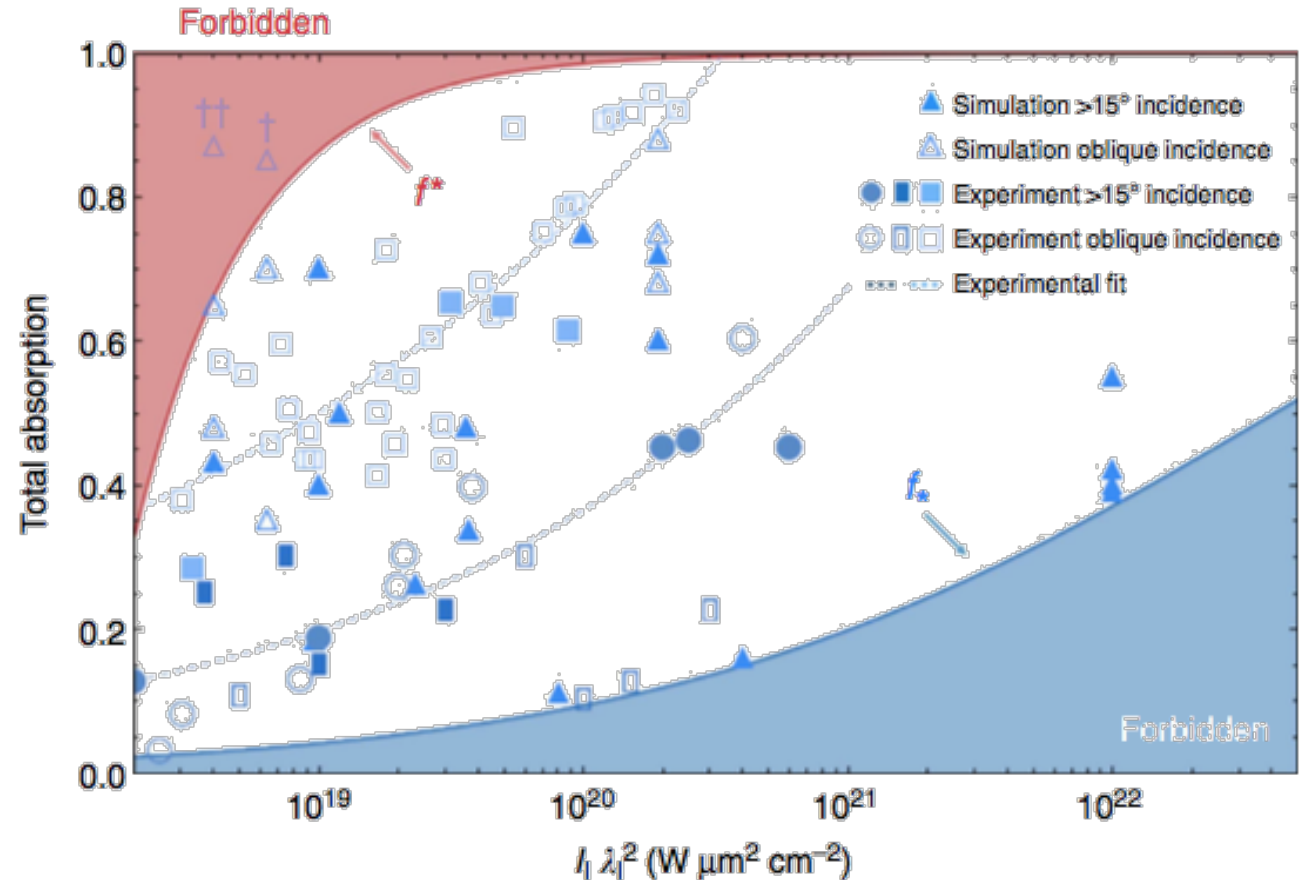
M. Murnane, Thesis, 1989



G. Doumy, et al., Phys. Rev. E **69** 1 (2004)

Absorption understanding

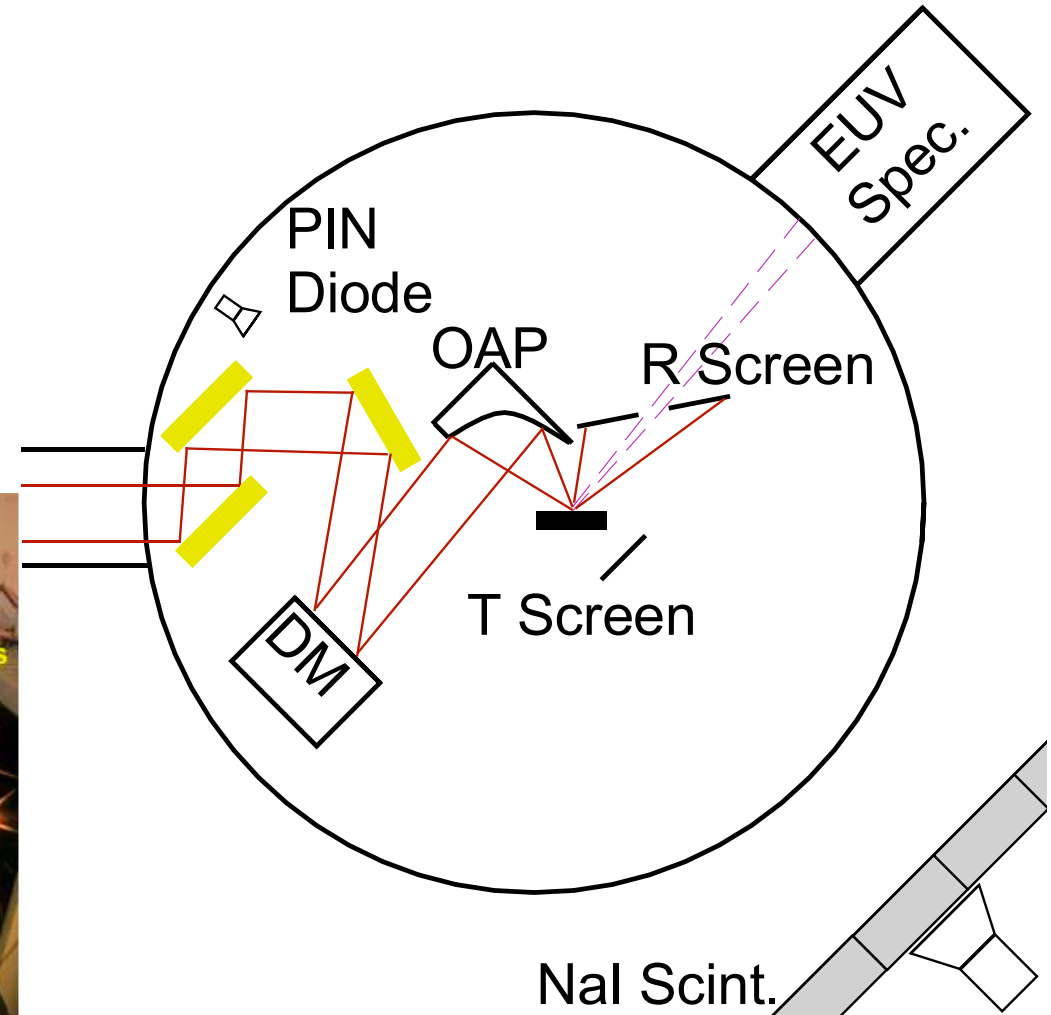
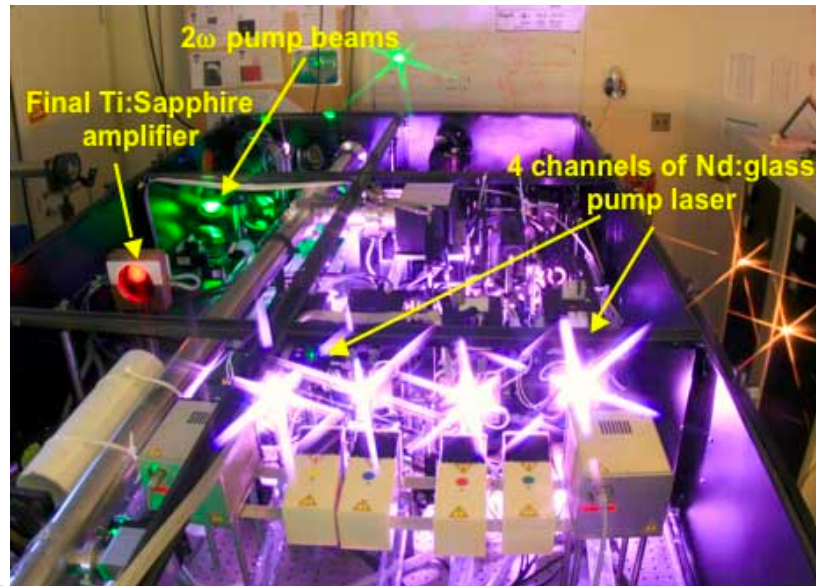
- Experiment and simulation shows large variation in absorption measurement
- Variables include:
 - Pulse duration
 - Polarization
 - Plasma density profile
 - Focal conditions



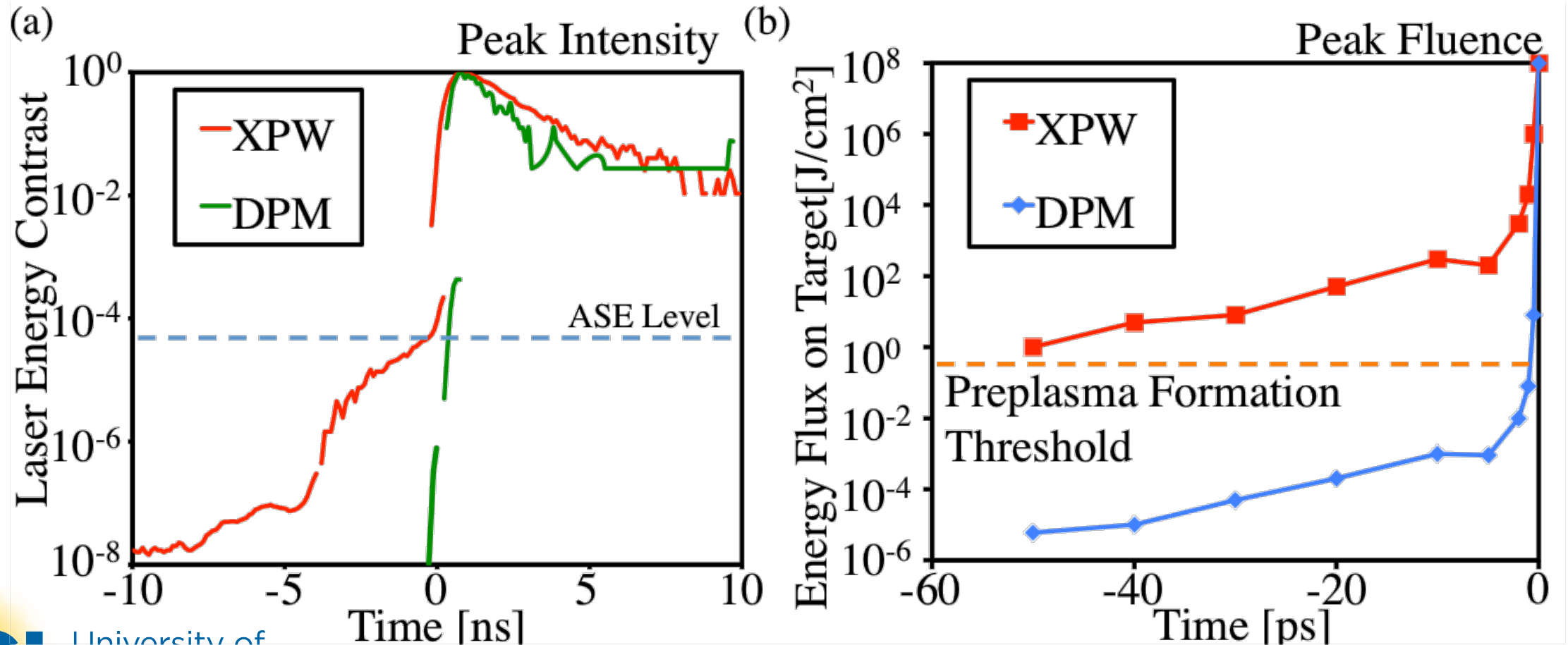
M. C. Levy, et al., Nat. Comm. 5, 4149 (2014)

Experimental setup

- HERCULES
 - 800 nm, 0.1 Hz
 - 30 fs
 - 1.5 J

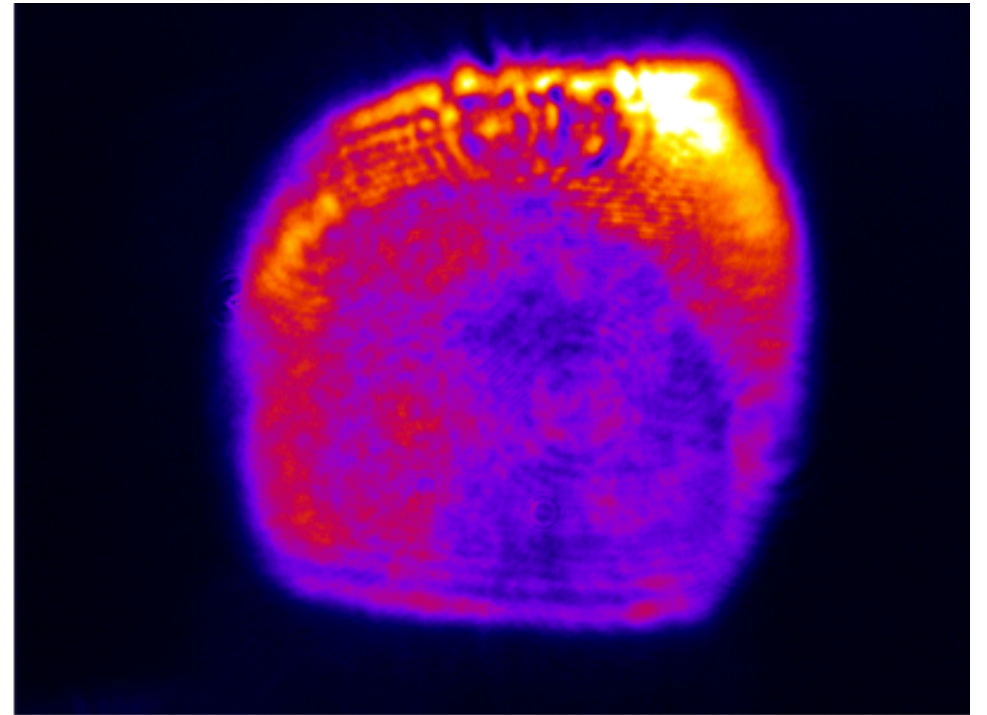
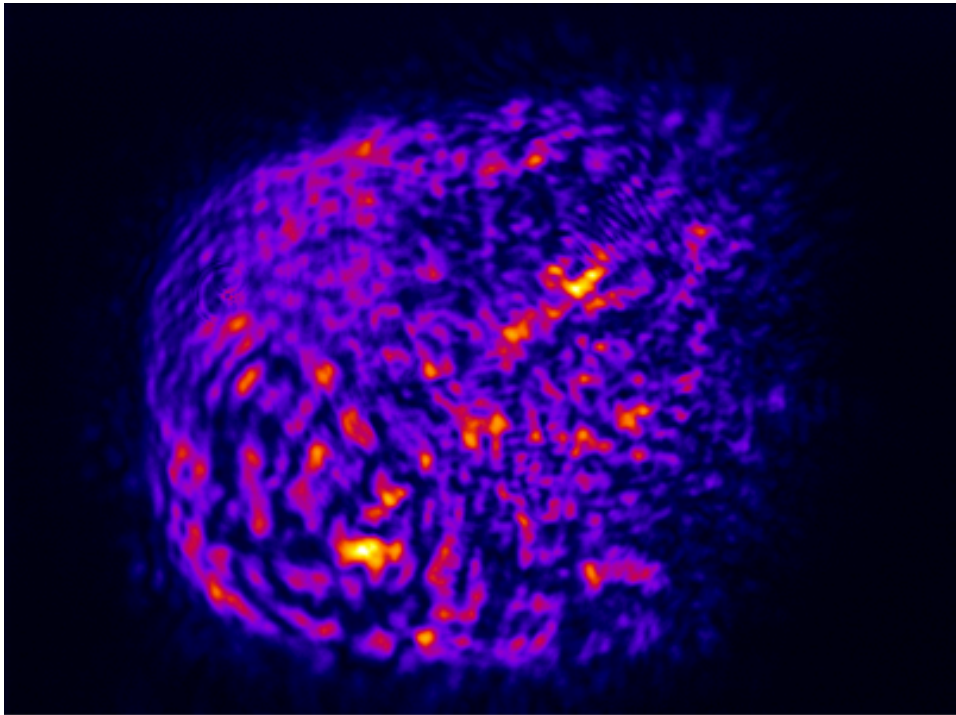


Pulse cleaning

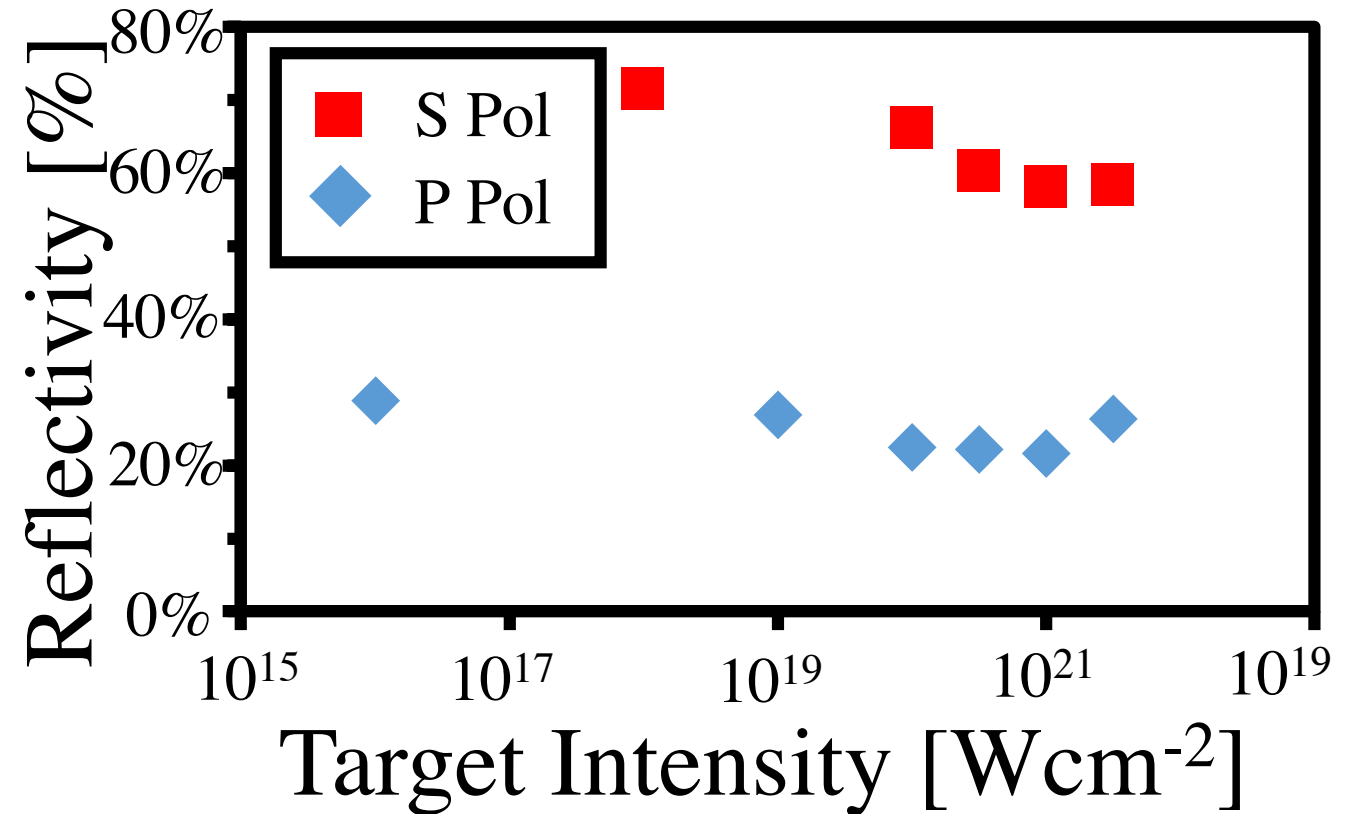
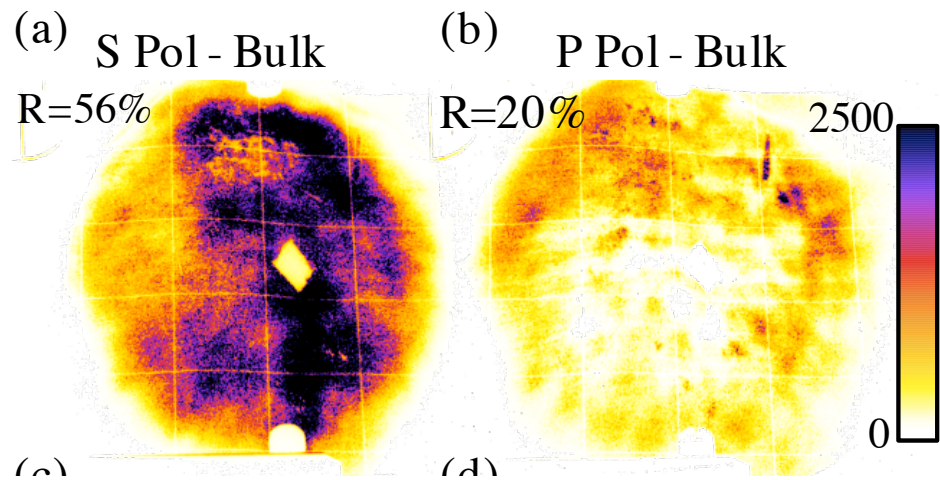


Contrast issues

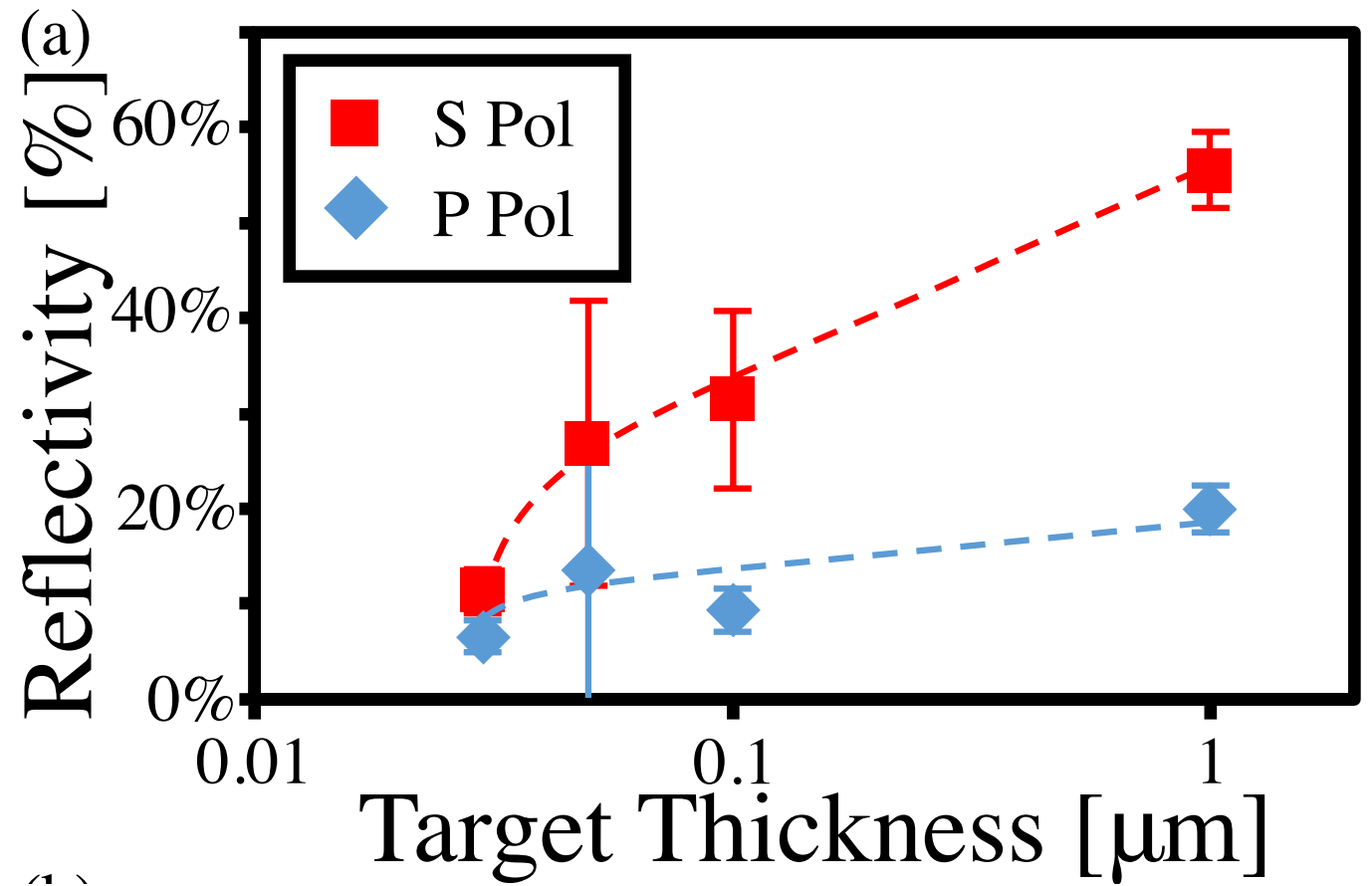
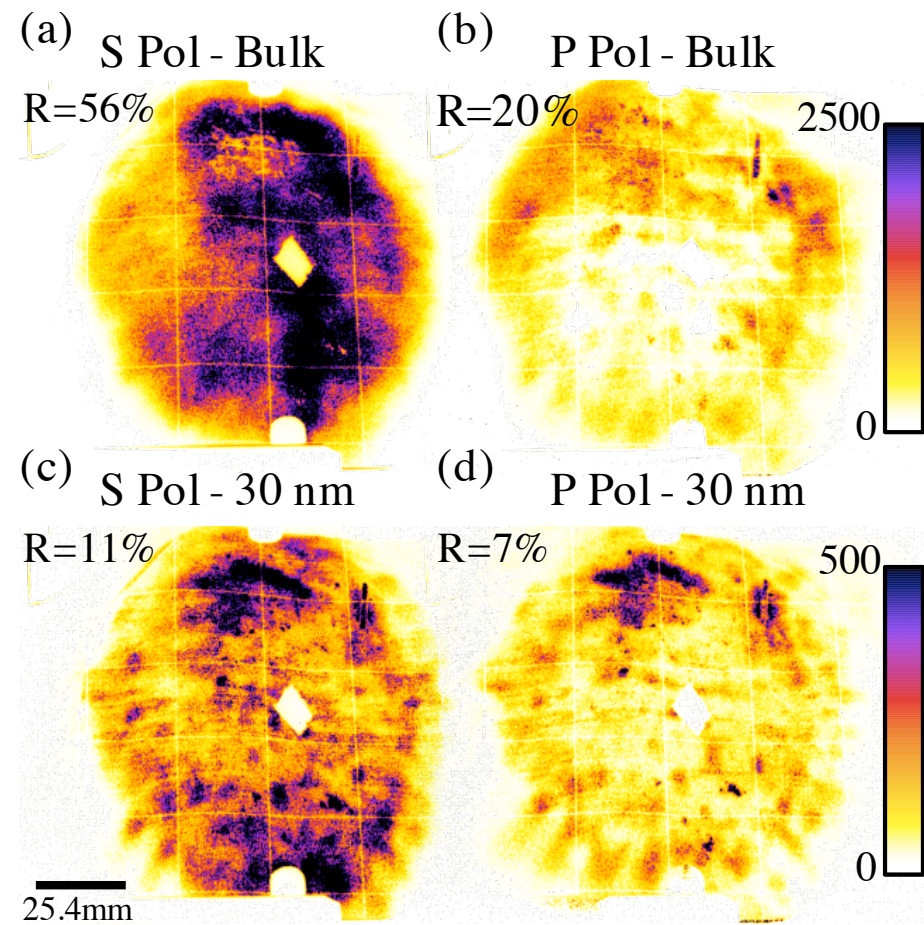
- XPW comparison between 10^{16} and 10^{15} plasma mirror



Polarization dependence



Polarization dependence

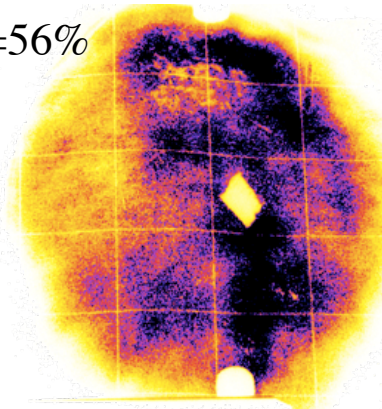


HHG with ion motion

- Harmonics were lost for thinner targets with modulated beam profiles
- Modulation at plasma surface prevents coherent buildup of x-rays

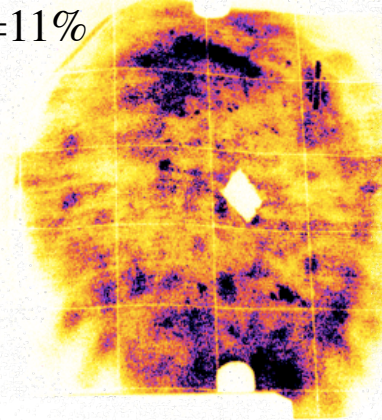
(a) S Pol - Bulk

R=56%

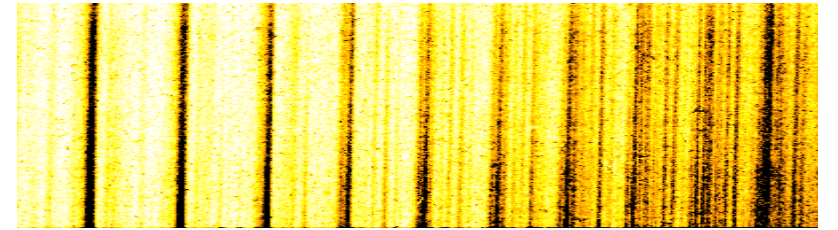


(c) S Pol - 30 nm

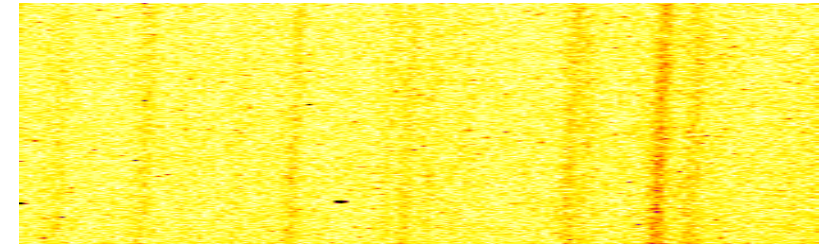
R=11%



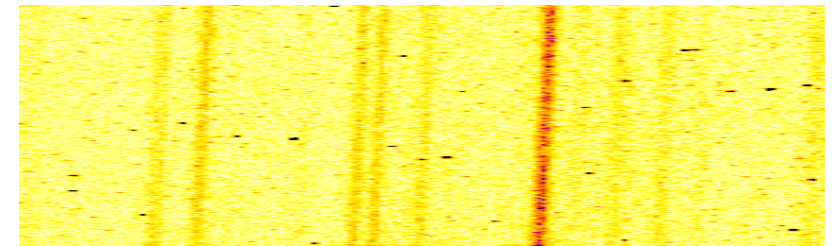
Bulk x-ray emission



1000 nm x-ray emission

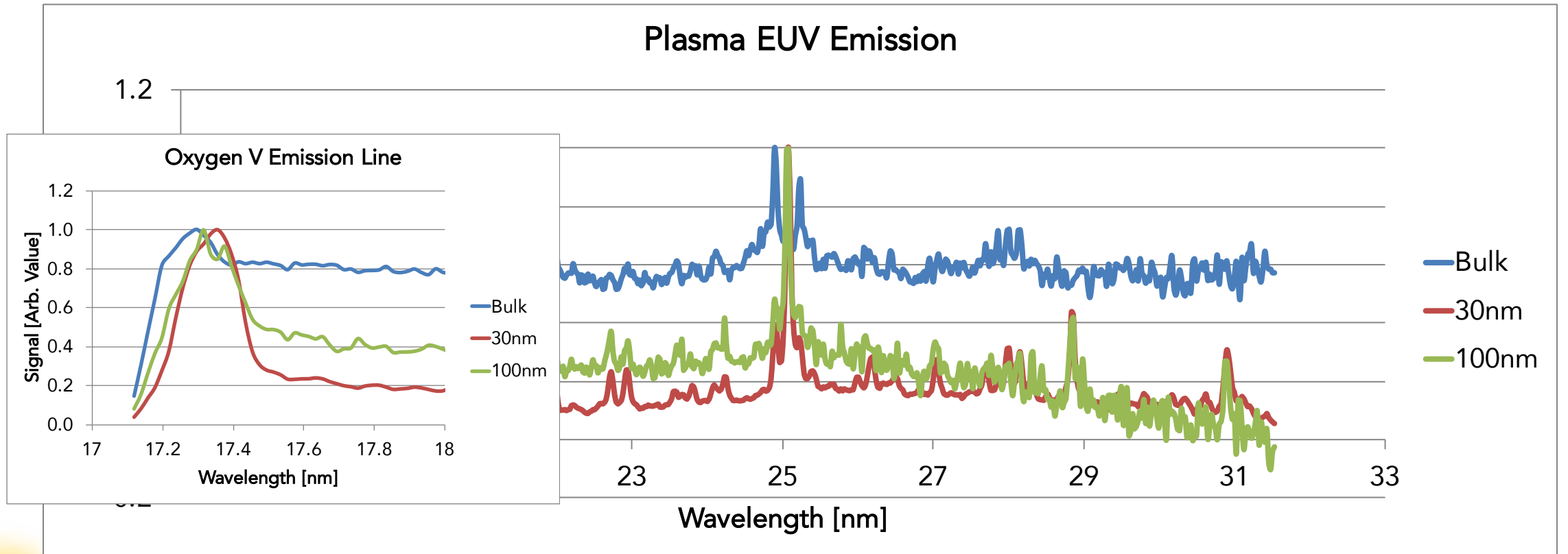


30 nm x-ray emission



Redshifting Oxygen Lines

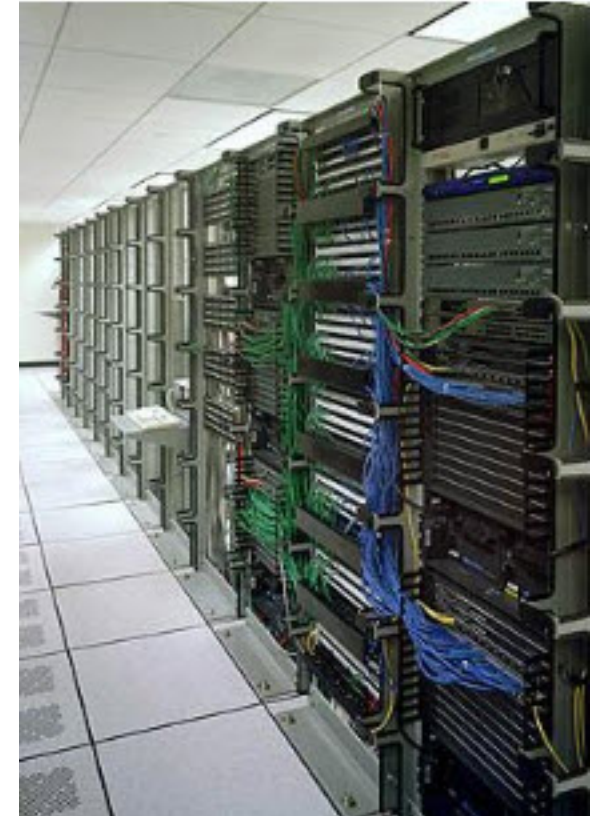
Plasma EUV Emission



PIC Simulation capabilities

- GreenPlanet computing cluster @UCI
- 592 Intel Xeon E5 cores
- 6 GB/core

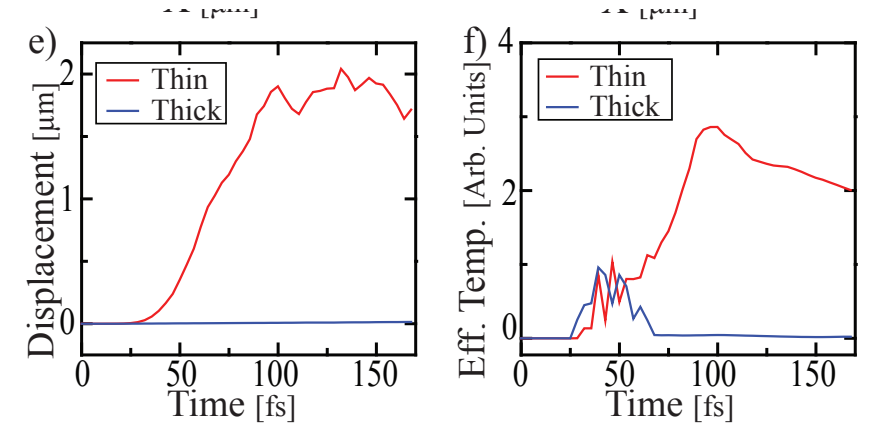
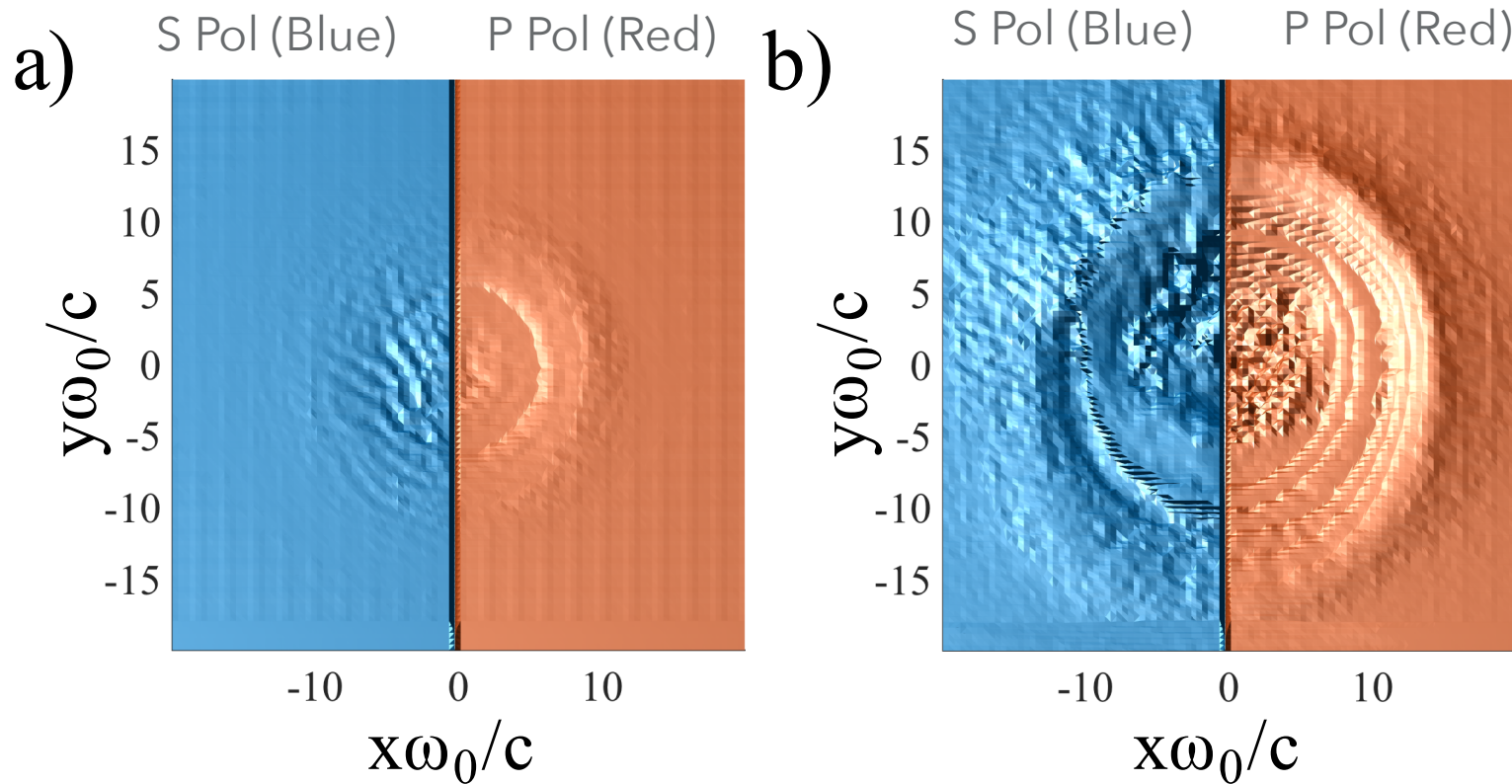
- Collaboration with PICKSC for simulation codes
 - OSIRIS 4.0 particle-in-cell
 - OSHUN VFP



We acknowledge the OSIRIS Consortium (UCLA/IST Portugal) for use of OSIRIS.

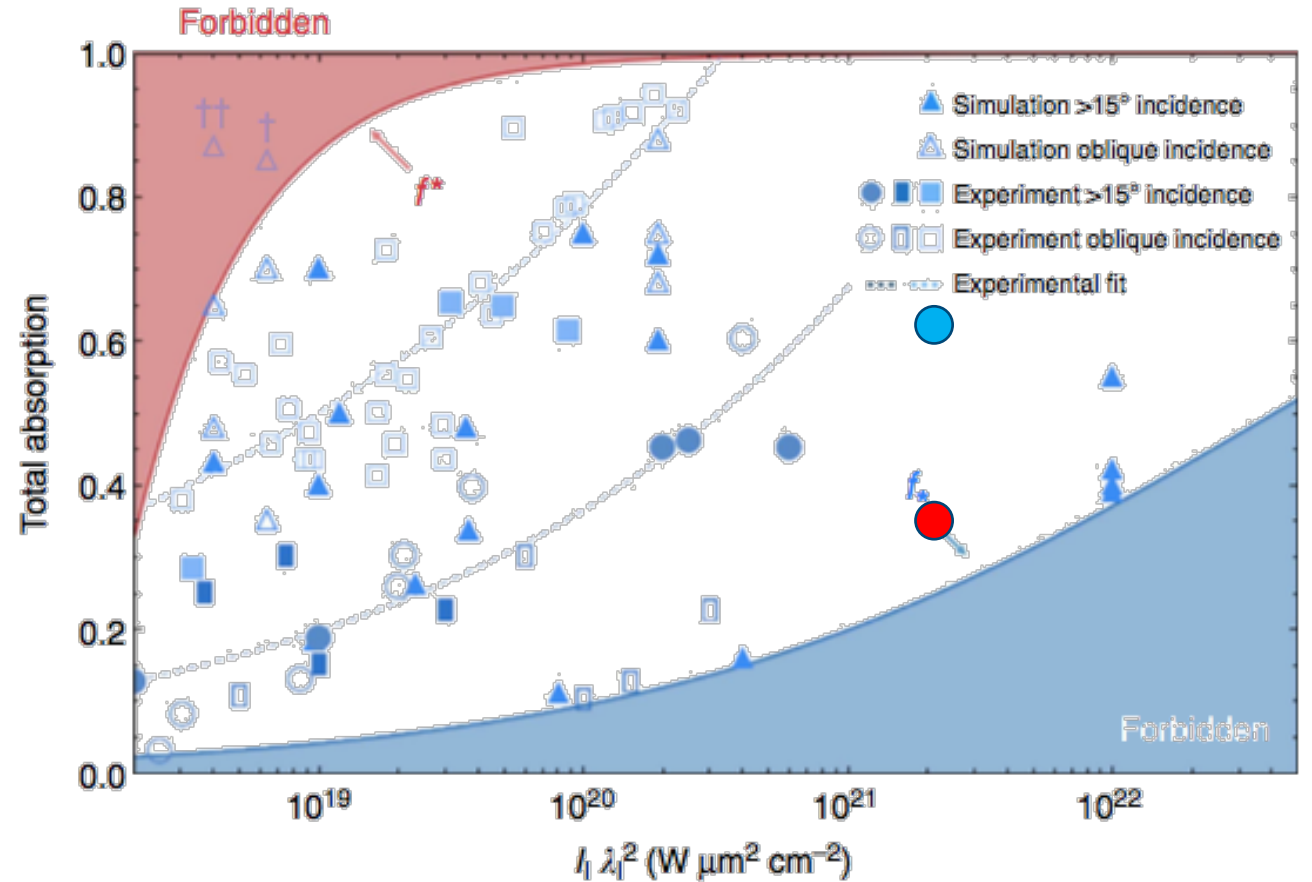
3D Simulations

F. Dollar, et al., New J. Phys. **19** 063014(2017)
F. Dollar, et al., PRL **108**, 175005 (2012)



Absorption understanding

- High contrast experiments
- Much lower absorption observed than general trends

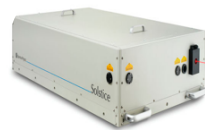


M. C. Levy, et al., Nat. Comm. 5, 4149 (2014)

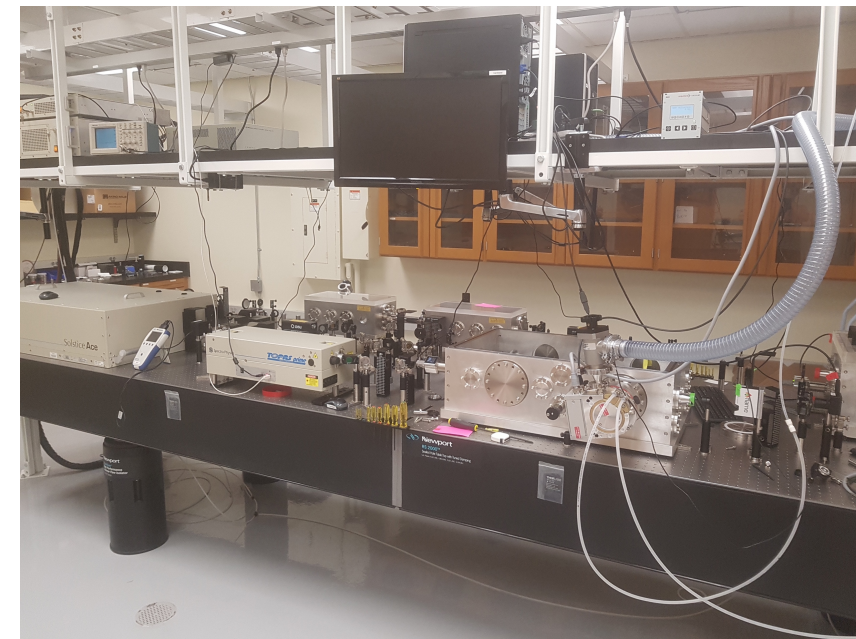
Relativistic HHG

- Fundamental questions remain
 - What is the relation between hot electron generation and HHG?
 - How do plasma conditions affect surface plasma waves?
 - Do single atom scalings hold for collective effects?
- Mid infrared provides unique experimental opportunities
 - Visible harmonics
 - Overdense targets
 - Higher a_0 for a given intensity

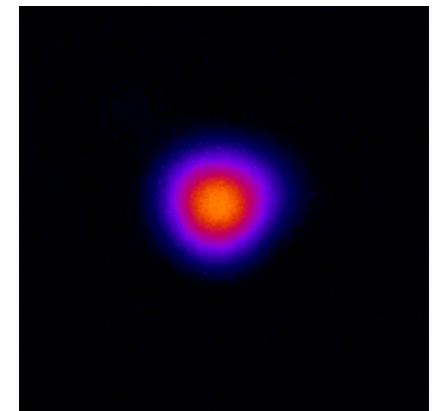
Experimental setup at UCI



Solstice ACE
800 nm
1 kHz, 7 mJ, 35 fs



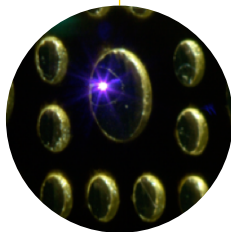
M squared < 1.1



4.17 μm measured
4.07 μm diffraction limit



Mid-Infrared
Beam
1300-2100 nm
1 kHz, 1.3/0.7 mJ,
40 fs



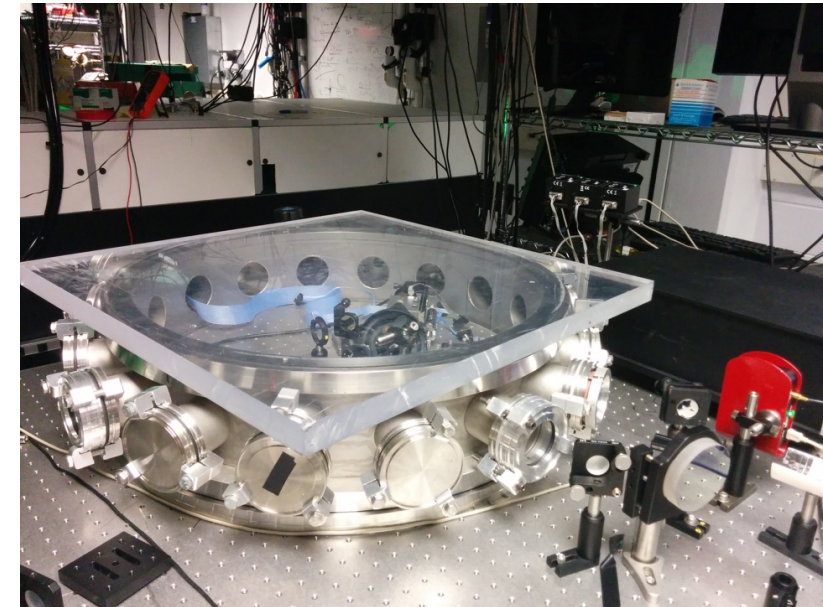
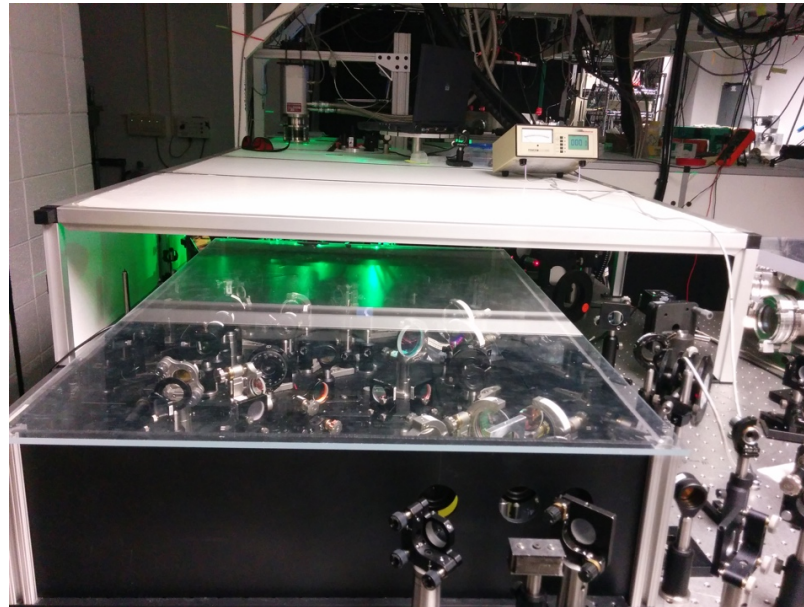
Probe Beams
2 x 800 nm
1 kHz, 1 mJ, 35 fs



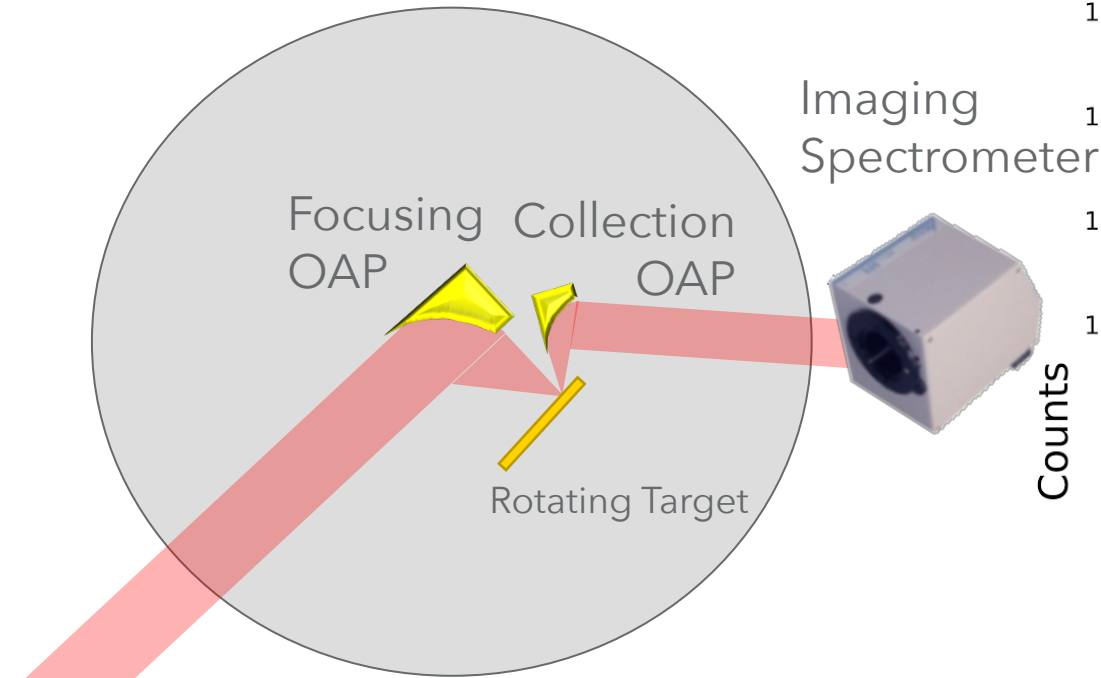
Femtokit
267-400 nm
1 kHz, 2 mJ, 35 fs

Experimental setup at Michigan

- Lambda Cubed
 - 800 nm, 0.5 kHz
 - 30 fs
 - 20 mJ
- 2 micron OPA
 - 35 fs
 - 2 mJ

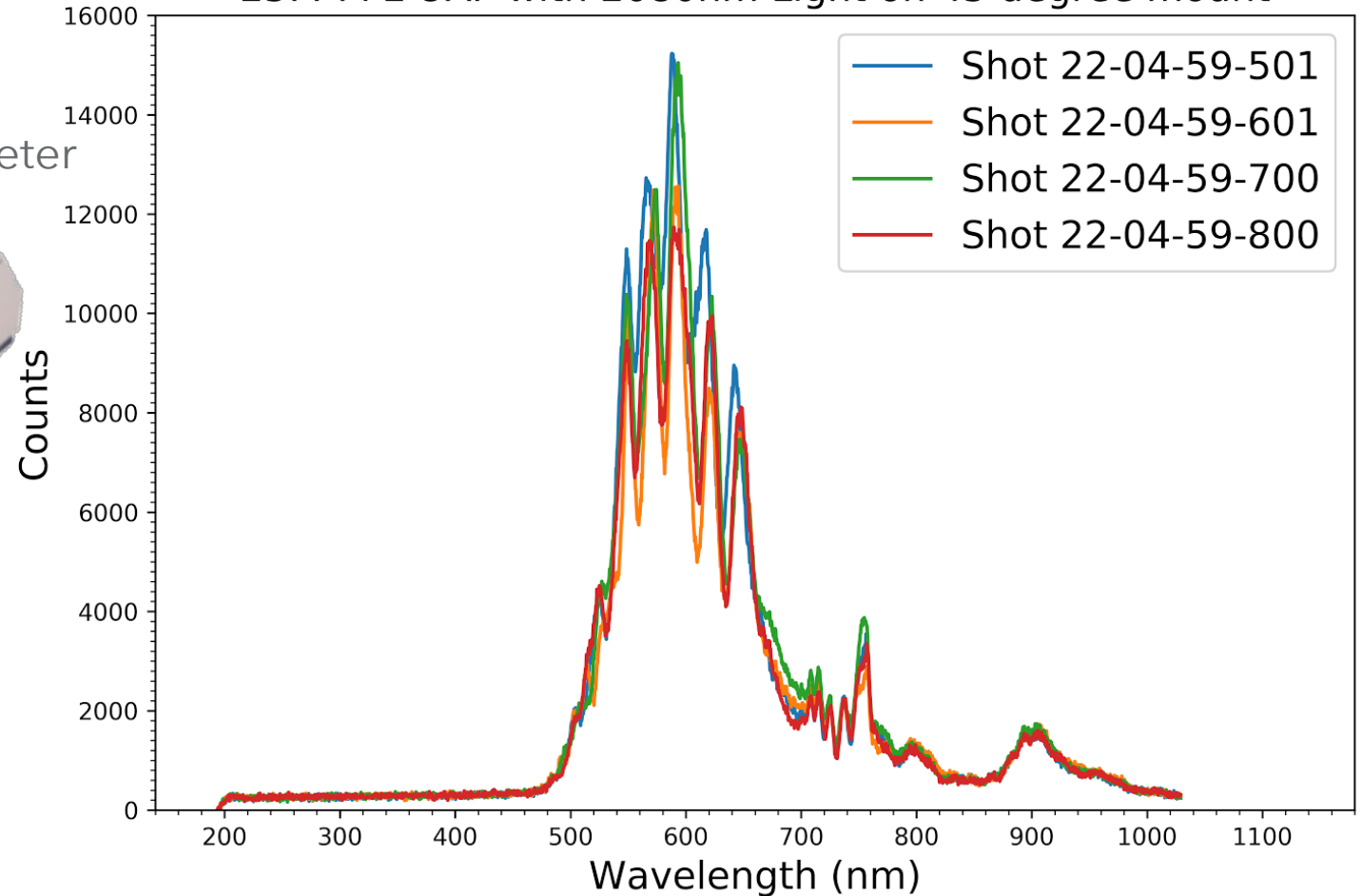


Low order harmonic emission

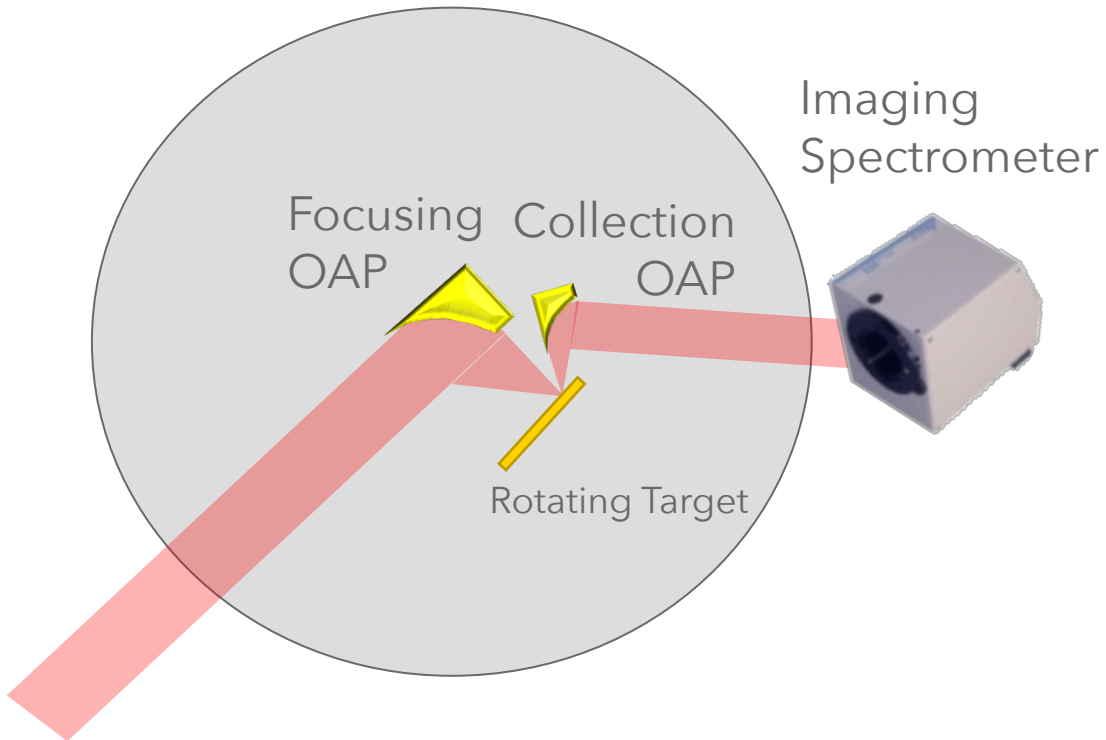


0.6 mJ 2050 nm delivered to target with $>10^{16}$ Wcm⁻²

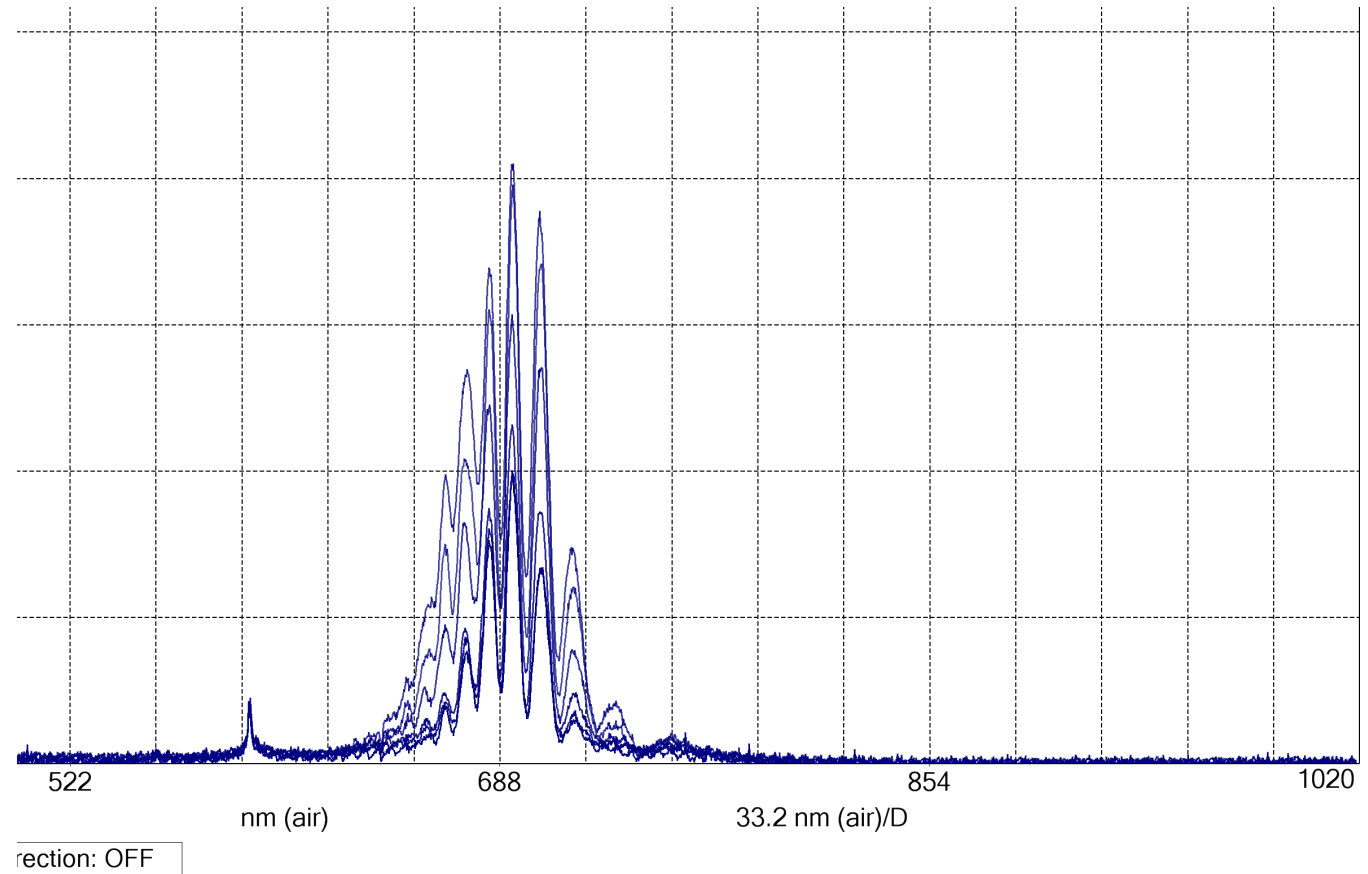
25.4 PFL OAP with 2080nm Light on 45 degree mount



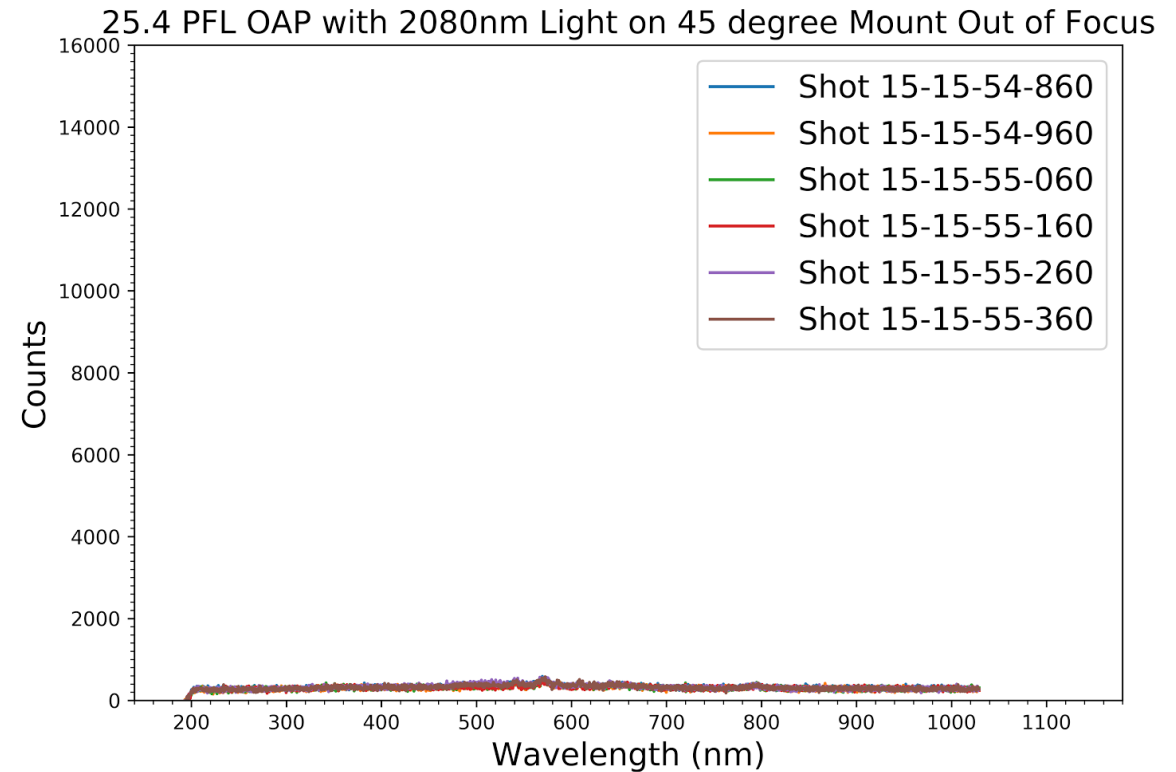
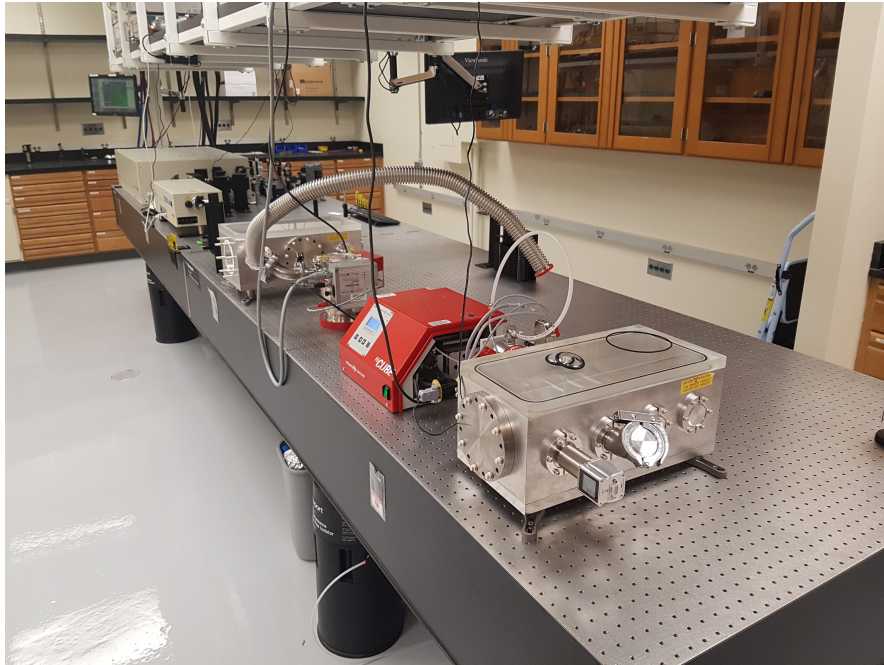
Low order harmonic



1.6 mJ 1950 nm delivered to target with $>10^{16}$ Wcm⁻²

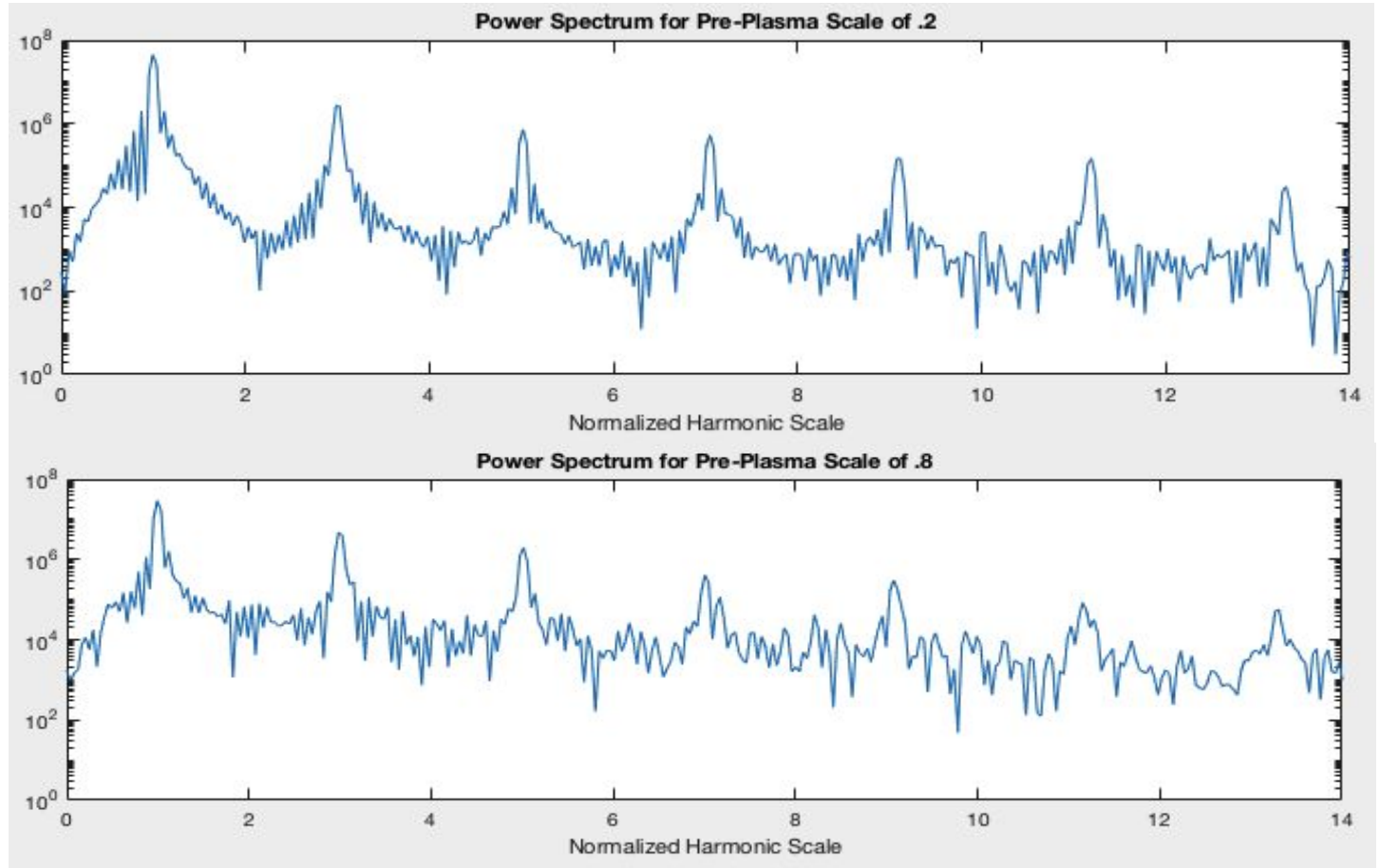


Low order harmonic emission



OSIRIS Simulation results

- OSIRIS 3D3V PIC Simulations
 - Reflected beam profiles
 - Incident beam $a_0=15$
 - Target density $60n_{\text{crit}}$

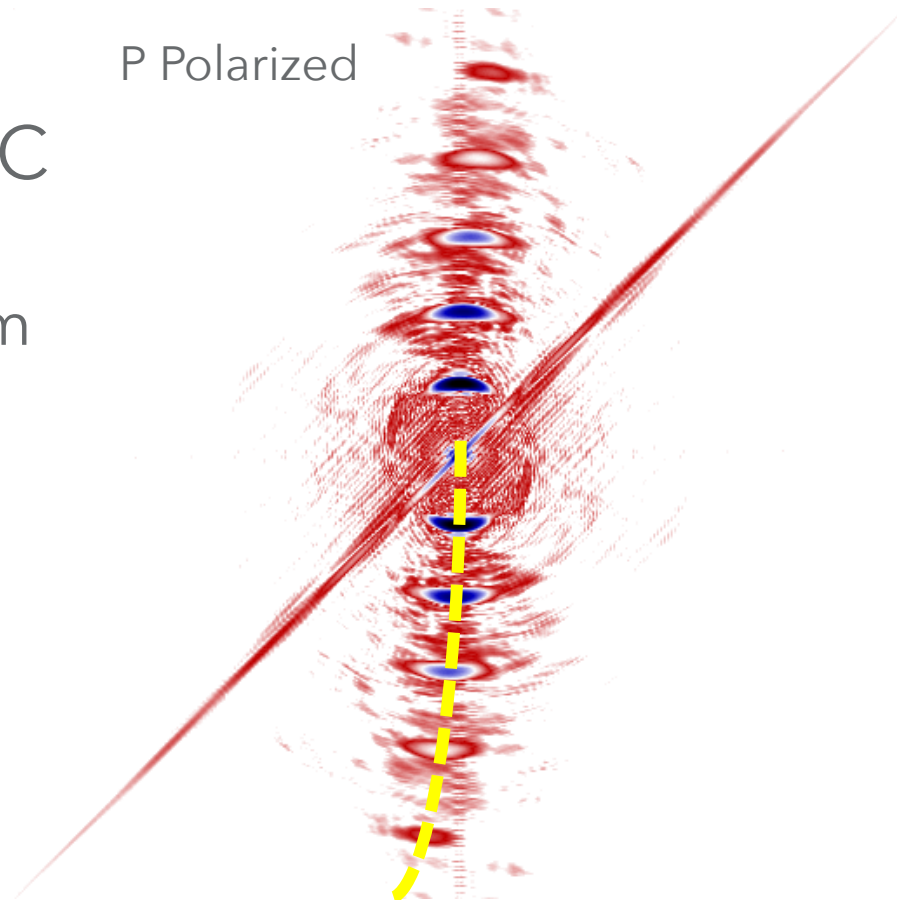


OSIRIS Simulation results

- OSIRIS 3D3V PIC Simulations

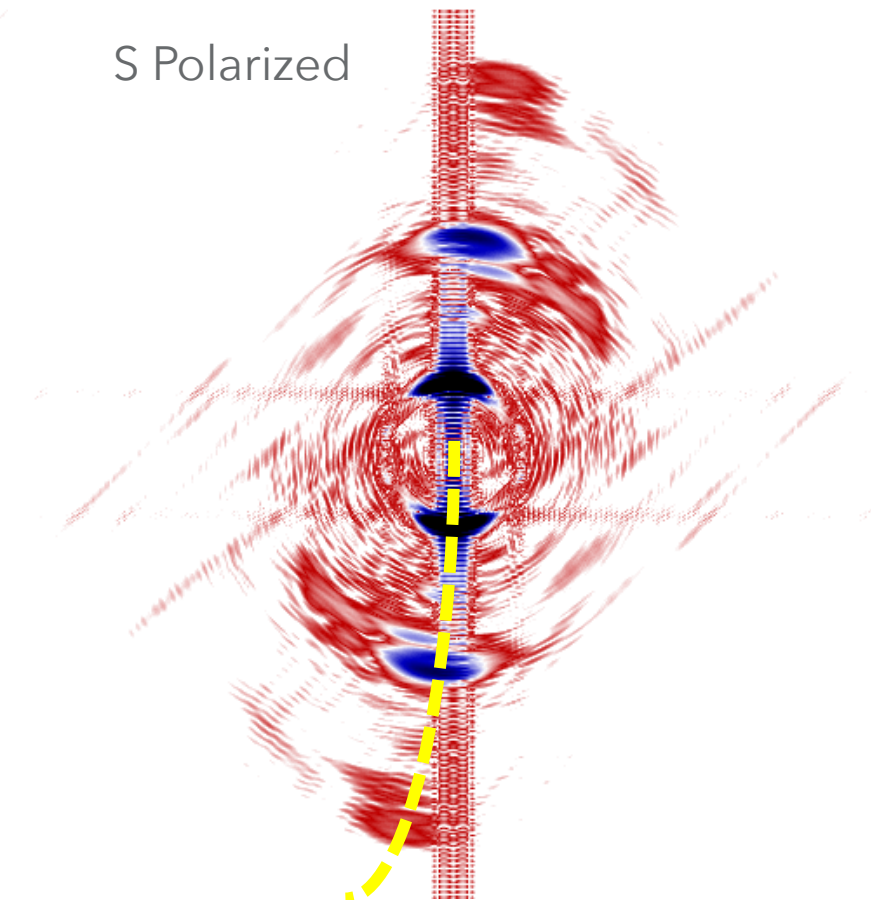
- Reflected beam profiles
- Incident beam $a_0=1$
- Target density $500n_{\text{crit}}$

P Polarized



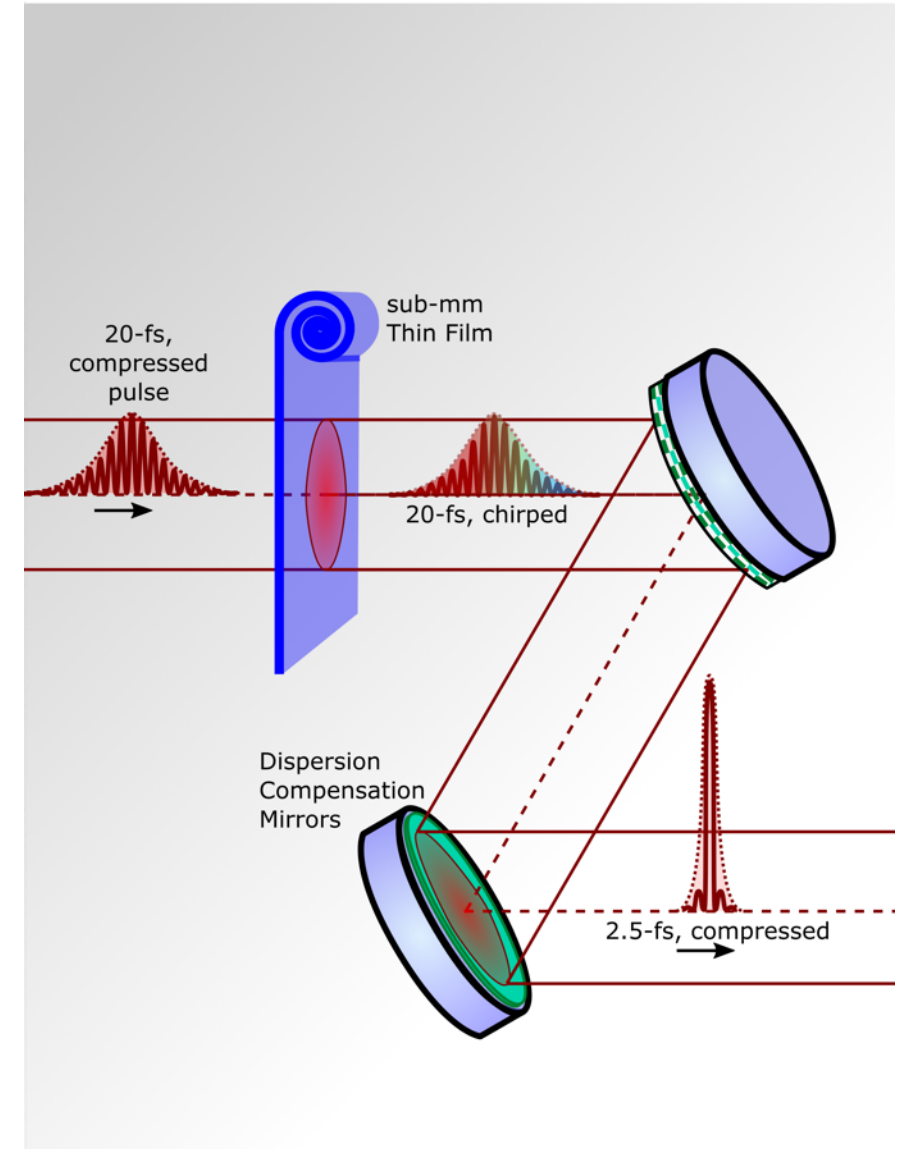
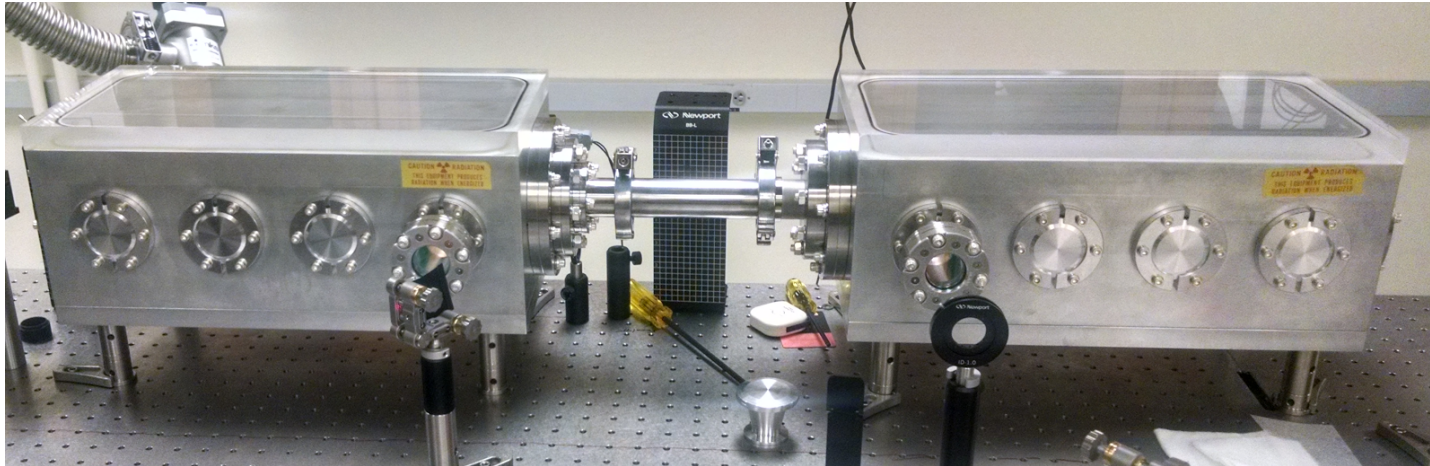
Fourier transform of Electric field x-direction

S Polarized

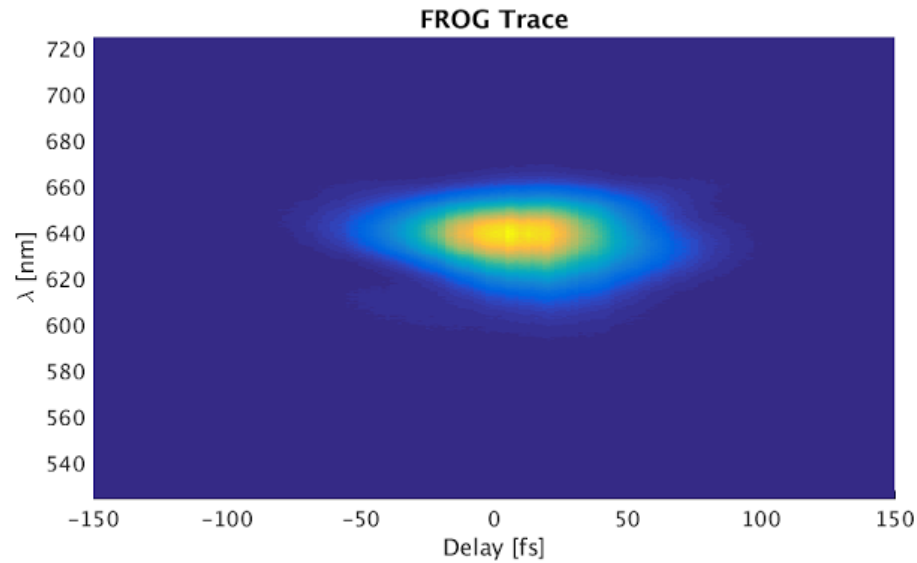


Fourier transform of Electric field z-direction

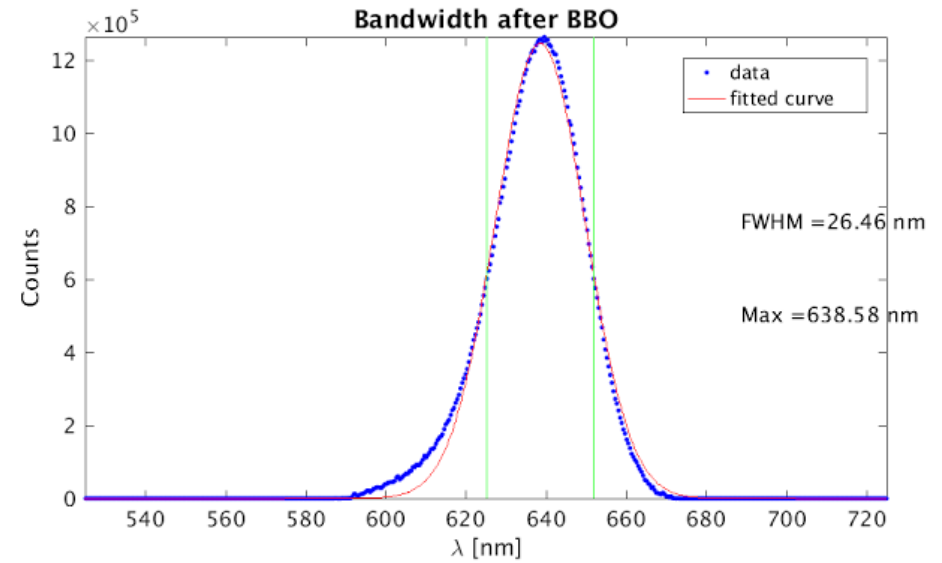
Thin film compression



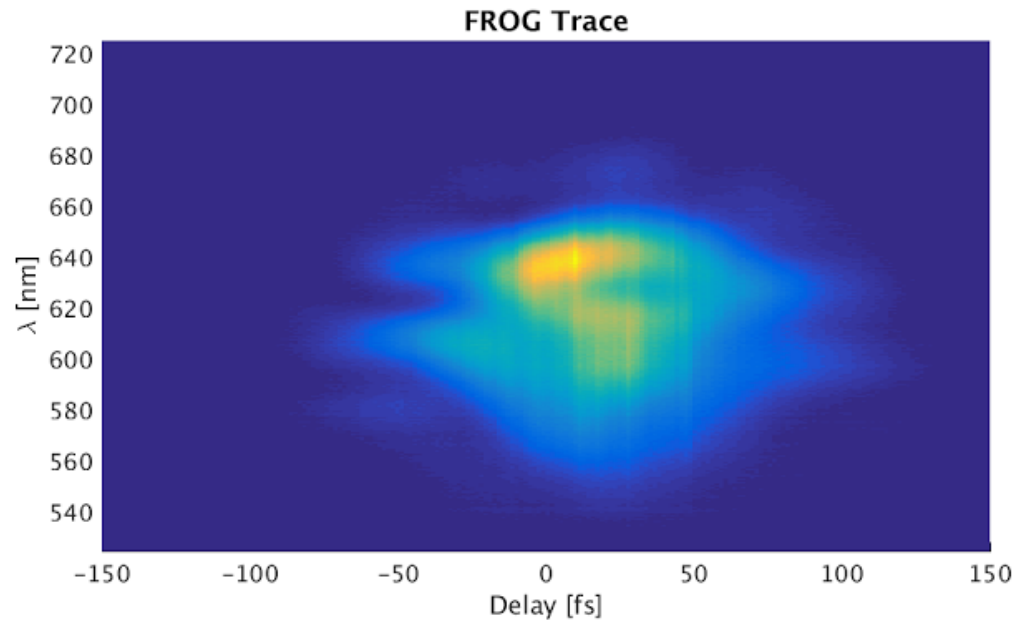
FROG trace



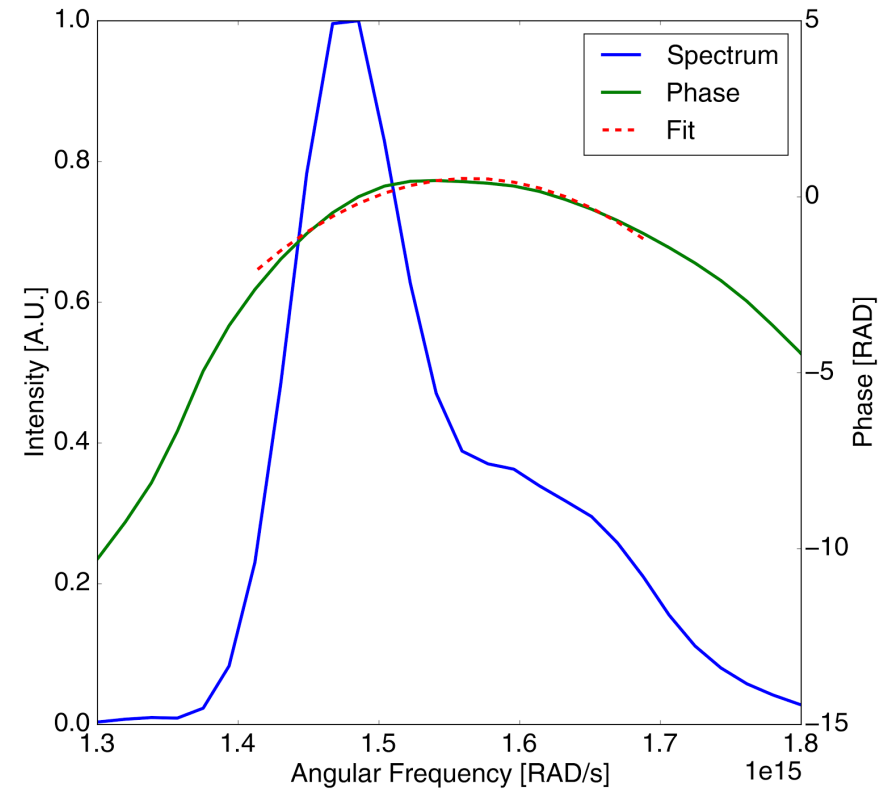
“standard” uncompressed beam



Compression at 1260

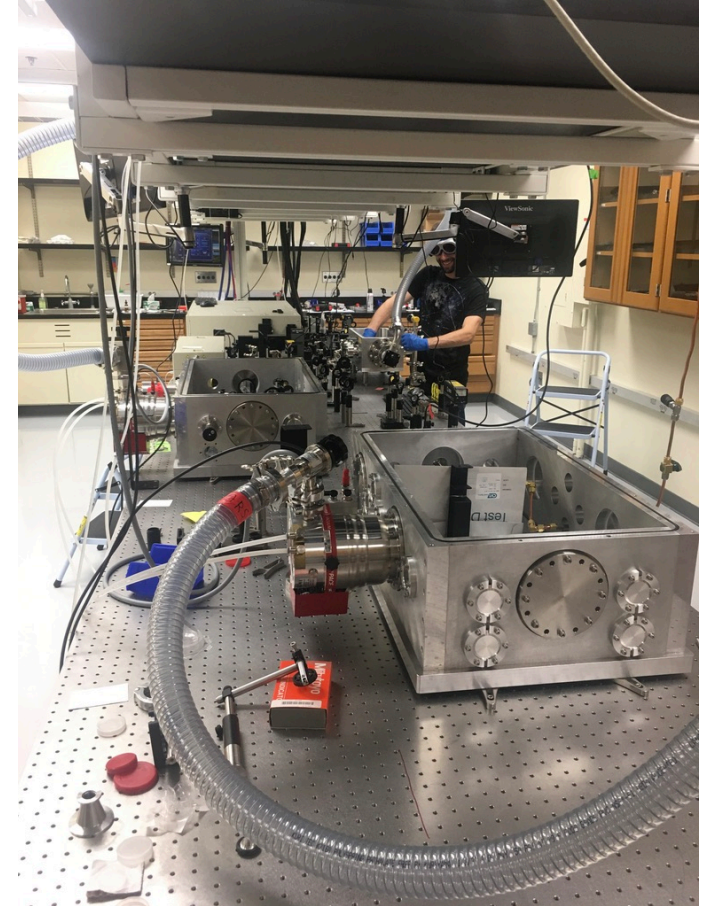


Reconstructed phase



Conclusions

- Laser driven, coherent X-ray probes offer a large number of opportunities
 - Supercontinuum for dynamic XAFS
 - High flux narrow lines for Thomson scattering
 - Circular polarization for dichroism
- High field harmonics offer additional advantages
 - Higher energy cutoffs and scalings
 - Information about laser solid interactions
- Ion motion increasingly complicates absorption



Acknowledgements

Thank you to Paul and Casi and to you for listening!

UCI

Tam Nguyen
Deano Farinella
Sahel Hakima
Hunter Allison
Matt Stanfield
Nick Beier
Cheyenne Nelson
Edgar Ibarra
Toshi Tajima

UCI School of
Physical Sciences



**Alfred P. Sloan
FOUNDATION**



Michigan group
(Karl Krushelnick &
Alec Thomas)



JILA group
(Margaret Murnane &
Henry Kapteyn)



STROBE
NSF SCIENCE AND TECHNOLOGY CENTER

UCI University of
California, Irvine